Radar microphysical retrievals and climatology of the vertical profiles of microphysical variables in different weather systems

Alexander Ryzhkov

University of Oklahoma, National Severe Storms Laboratory

Motivation

- The need to provide extensive observational reference for cloud modelers beyond very limited in situ microphysical data collected during field campaigns
- The need to improve microphysical parameterization in the NWP models using polarimetric radar observations
- The need to assimilate radar-derived microphysical parameters of hydrometeors to the NWP models
- The need for better quantification of precipitation using radar measurements (snow in particular)
- Recently introduced techniques for processing and visualization of the vertical profiles of radar variables and microphysical parameters such as QVP, RD-QVP, and CVP provide very efficient representation of the vertical storm structure and its evolution

Key microphysical parameters to be determined

- Liquid water content of rain and snow / ice (LWC / IWC) (g m^{-3})

- Mean volume diameter $D_m = M_4/M_3$ (mm)

- Total number concentration N_t (L^{-1})

Radar estimates of liquid water content LWC

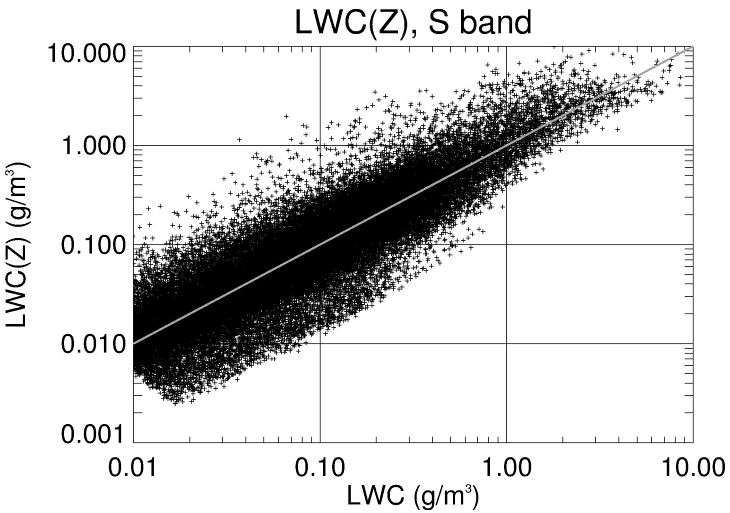

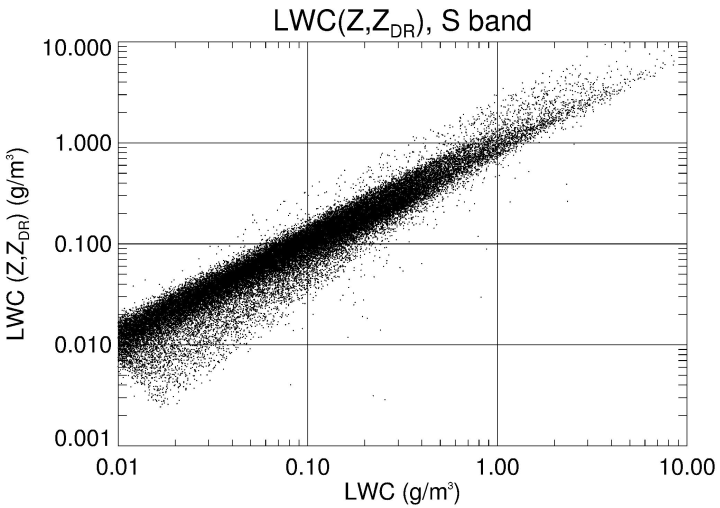

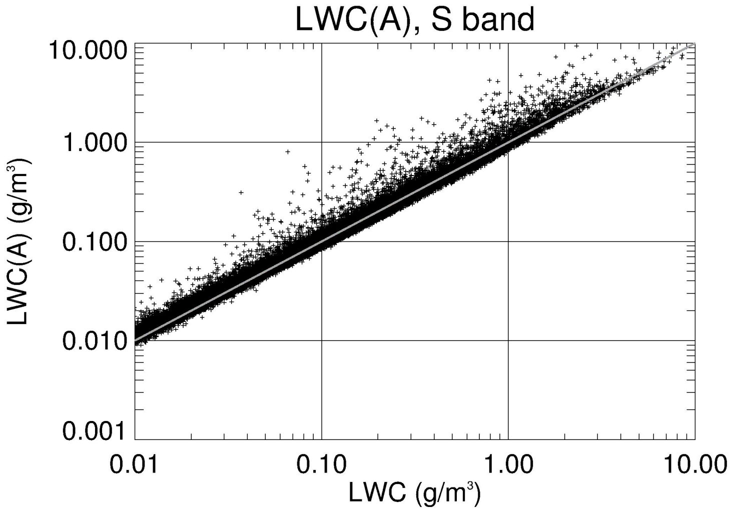

S band

$$LWC(Z) = 1.74\,10^{-3}\,Z^{0.64}$$

$$LWC(Z, Z_{DR}) = 1.38\,10^{-3}\,Z\,10^{(-2.43 Z_{DR} + 1.12 Z_{DR}^2 - 0.176 Z_{DR}^3)}$$

$$LWC(A) = 115\,A^{0.92}$$

$[Z] = mm^6 m^{-3}$, $[Z_{DR}] = dB$, $[A] = dB/km$, $[LWC] = \text{deg}/km$

Estimation of the mean volume diameter of raindrops D_m

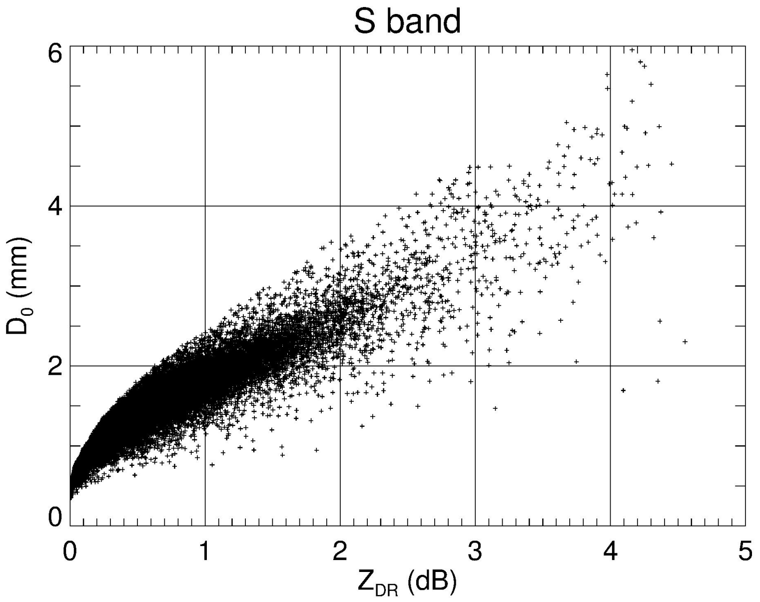

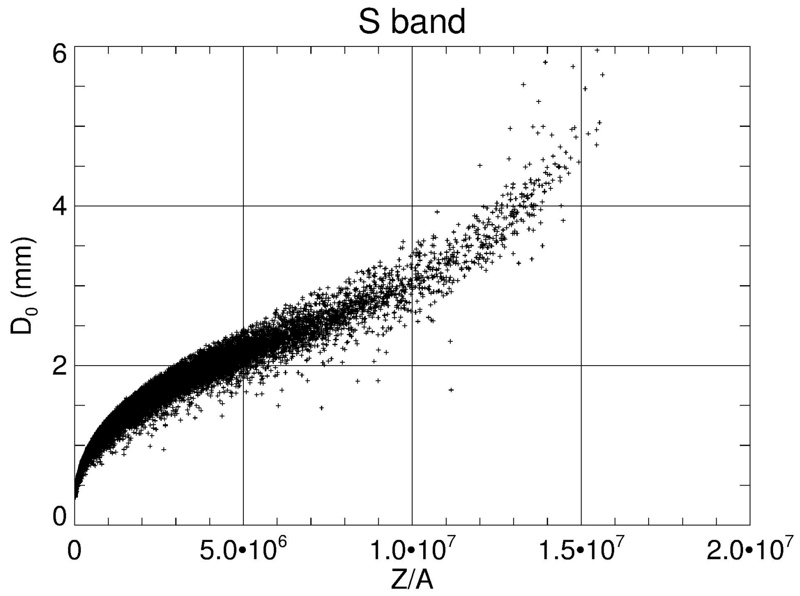

Bringi and Chandrasekar (2001)

$$D_m = 1.62\ Z_{DR}^{0.49}$$

Bringi et al. (2002)

$$D_m = 1.97\ Z_{DR}^{0.49}$$

Brandes et al. (2002)

$$D_0 = 0.171 Z_{DR}^3 - 0.725 Z_{DR}^2 + 1.48 Z_{DR} + 0.717$$

S band

T = 20°

$$D_m = 0.630 + 0.675x - 0.124x^2 + 0.0115x^3 - 0.00034x^4$$

$$x = \frac{Z}{A} 10^{-6}$$

$$[Z] = mm^6 m^{-3}, \quad [Z_{DR}] = dB, \quad [A] = dB/km, \quad [D_m] = mm$$

Caveats: Z_{DR} should be well calibrated, A is a function of radar wavelength and temperature

Estimation of the total number concentration of raindrops N_t

$$\log(N_t) = -2.37 + 0.1Z - 2.89Z_{DR} + 1.28Z_{DR}^2 - 0.213Z_{DR}^3$$

Z is expressed in dBZ, Z_{DR} is in dB, and N_t is in L^{-1}

Relations for polarimetric microphysical retrievals in ice

(1) $$IWC(K_{DP}, Z_{DR}) = 4.0\times10^{-3}\frac{K_{DP}\lambda}{1-Z_{dr}^{-1}}$$

(2) $$IWC(K_{DP}, Z) = 3.3\times10^{-3}(K_{DP}\lambda)^{0.67}Z^{0.33}$$

(3) $$D_m(K_{DP}, Z_{DP}) = -0.1 + 2.0\left(\frac{Z_{DP}}{K_{DP}\lambda}\right)^{1/2}$$

(4) $$D_m(K_{DP}, Z) = 0.67\left(\frac{Z}{K_{DP}\lambda}\right)^{1/3}$$

(5) $$\log(N_t) = 3.39 + 2\log(IWC) - 0.1Z(dBZ)$$

$$\rho_s = \alpha D^{-1}$$

$$Z_{dr} = 10^{0.1 Z_{DR}(dB)}$$

$$Z_{DP} = Z_H - Z_V$$

λ is the radar wavelength in mm
Z is in mm^6m^{-3}
Z_{DP} is in mm^6m^{-3}
K_{DP} is in deg/km
IWC is in g m^{-3}
D_m is in mm
N_t is in L^{-1}

Eqs. (1) and (3) are utilized if $Z_{DR} > Z_{DR}^{(t)}$ and Eqs (2) and (4) are used otherwise ($Z_{DR}^{(t)}$ = 0.4 dB)

Estimates (1) and (3) are immune to the variability of the particles' shapes and orientations

Assumptions and limitations

- Rain retrieval relations have been obtained for S band based on the simulations using large DSD dataset obtained in Oklahoma
- Ice retrieval relations have been derived assuming that snowflake / crystals is the dominant habit and high-density graupel /hail is absent
- Some of the ice retrieval relations are derived with certain assumptions about particle shape, orientations, and degree of riming
- Ice particles are assumed to be Rayleigh scatterers
- Ice retrieval relations are valid if a single habit dominates the mixture
- All retrievals are valid for particles larger than 0.05 – 0.1 mm
- Additional microphysical retrievals are possible in convective downdrafts but not updrafts

$\rho_s(D) = 0.917\ g/cm^3$ D < D$_t$ < 1 mm $IWC \sim M_3$ $Z \sim M_6$ $K_{DP} \sim M_3$ $IWC \sim K_{DP}$

$\rho_s(D) = 0.1\ f_{rim} D^{-1}$ D > D$_t$ $f_{rim} = 1/(1-FR)$ FR is rime mass ratio $IWC \sim M_2$ $Z \sim M_4$ $K_{DP} \sim M_1$

Estimation of the mean volume diameter using dual-wavelength ratios (DWR)

DWR (S, Ka)

$$DWR(S, Ka) = 44.9 D_m^{1.72}$$

Courtesy of Sergey Matrosov

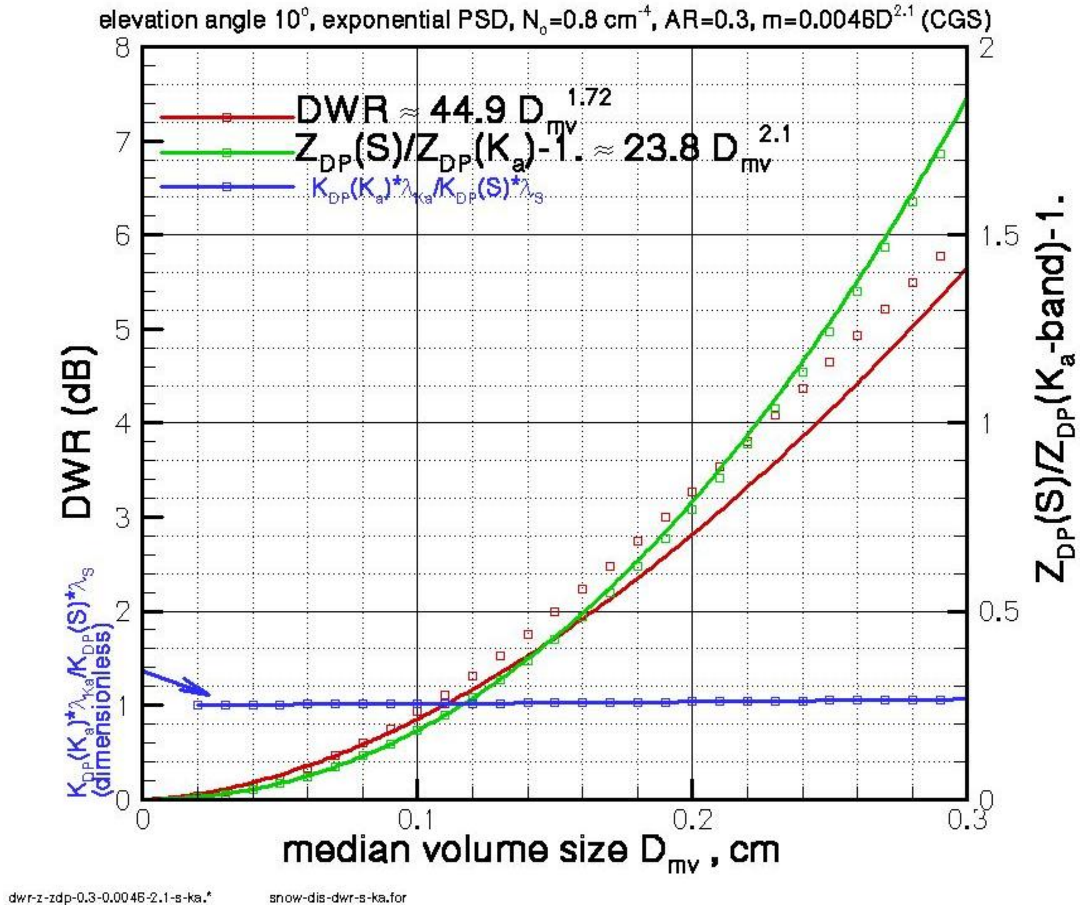

DWR (X, W)

Summary of all ICICLE flights

Matrosov et al. 2022

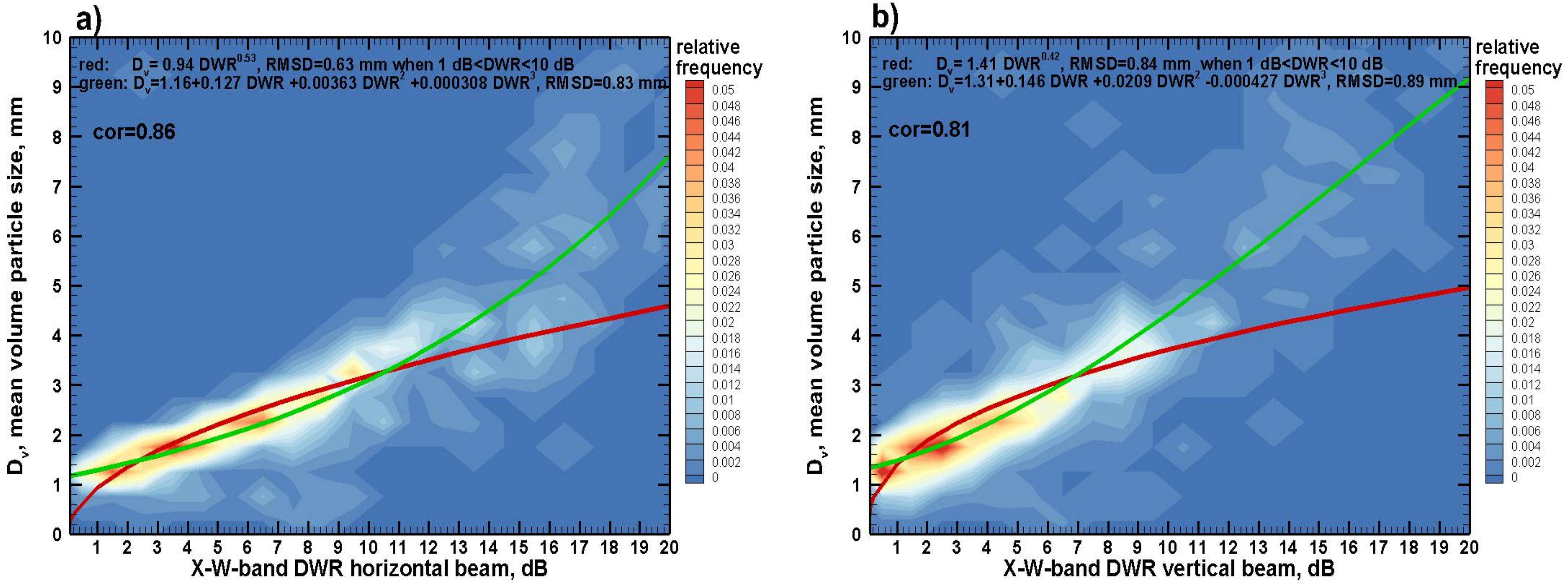

$$D_m = 1.16 + 0.127\, DWR + 0.0063\, DWR^2 + 0.000308\, DWR^3$$

$$D_m = 1.31 + 0.146\, DWR + 0.0209\, DWR^2 + 0.000427\, DWR^3$$

Microphysics of landfalling hurricanes

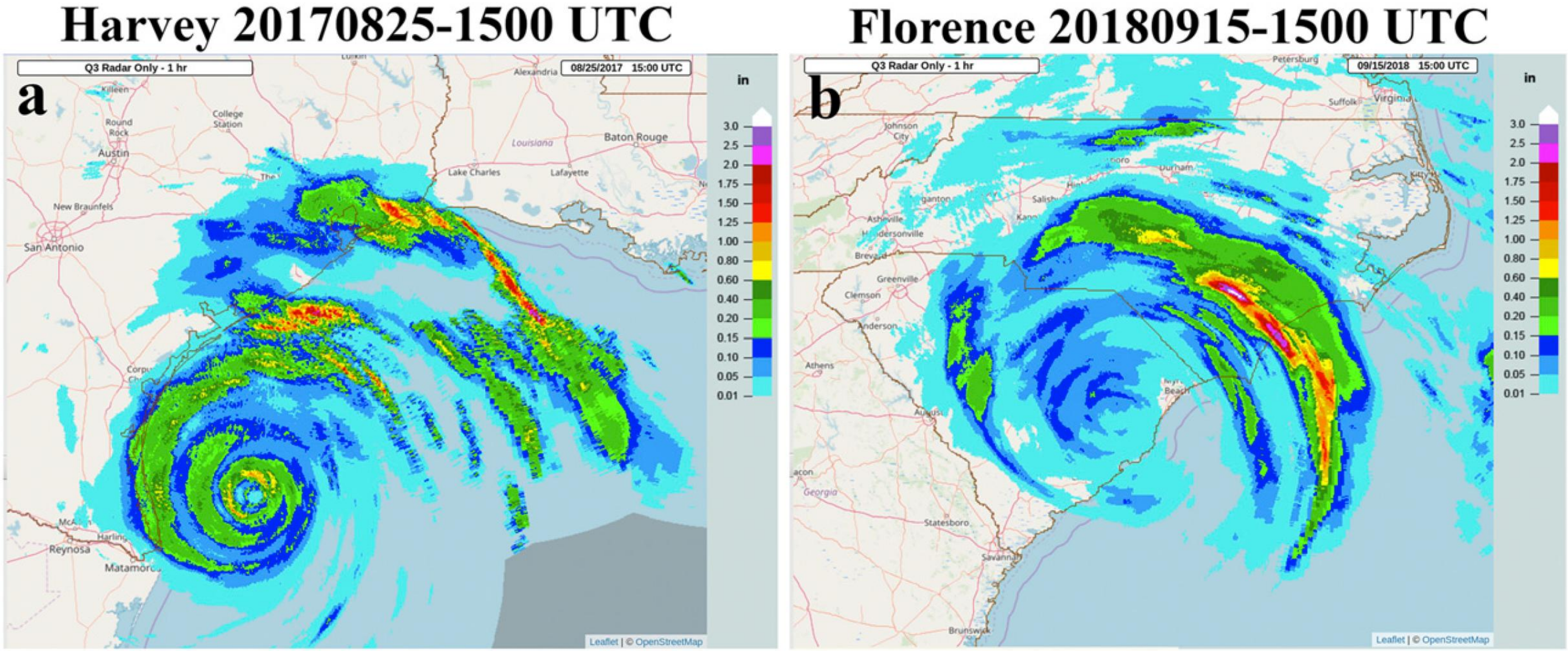

FIG. 3. The 1-h cumulative radar QPEs from MRMS for (a) Harvey for 1500–1600 UTC 25 Aug 2017 and (b) Florence for 1500–1600 UTC 15 Sep 2018

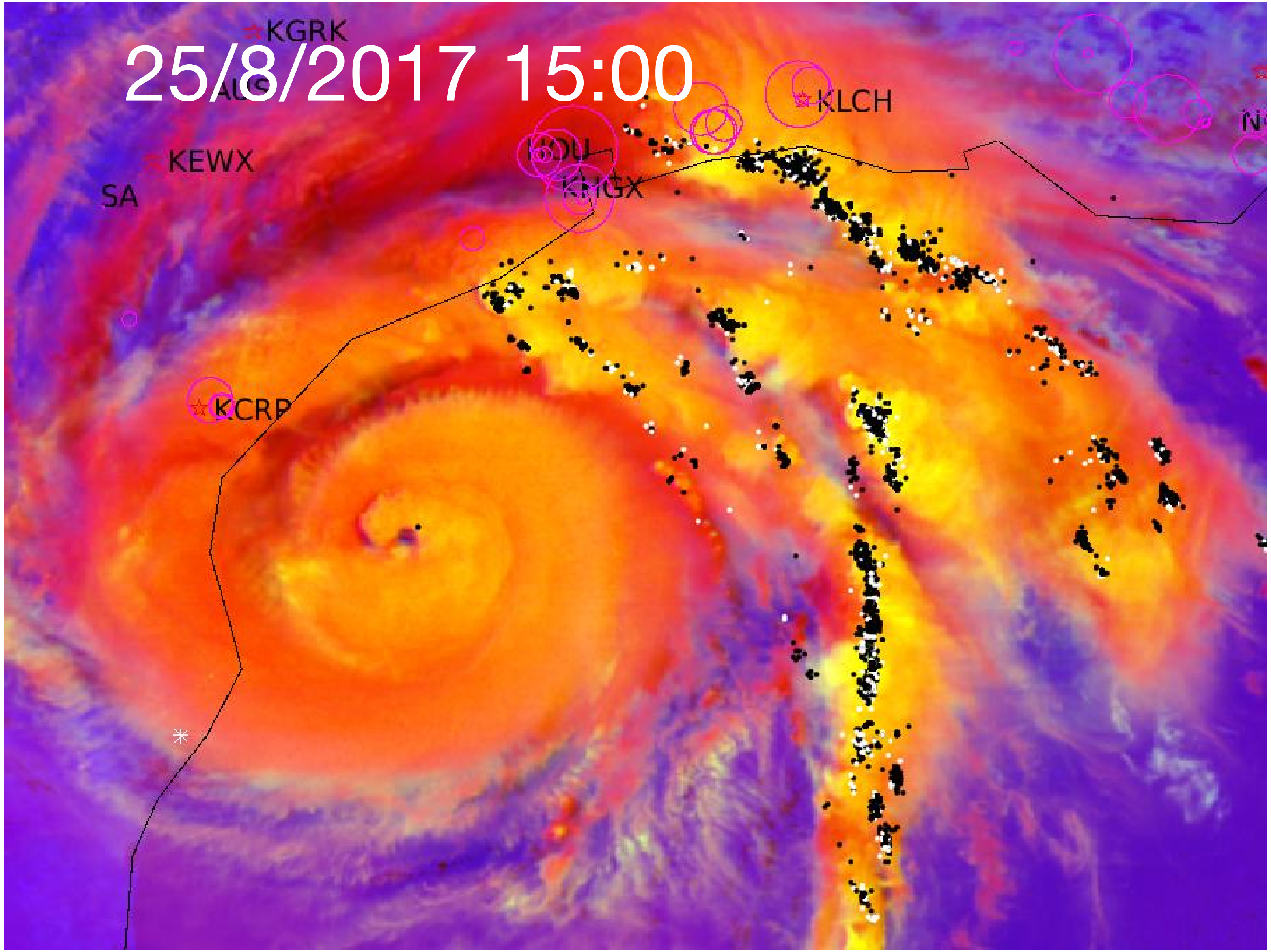

Integration of the polarimetric radar, satellite, and lightning information

Hu, J., D. Rosenfeld, A. Ryzhkov, and P. Zhang, 2020: Synergetic use of the WSR-88D radars, GOES-R satellites, and lightning sensors to study microphysical characteristics of hurricanes. *J. Appl. Meteor. Clim.*, **59**, 1051 – 1068.

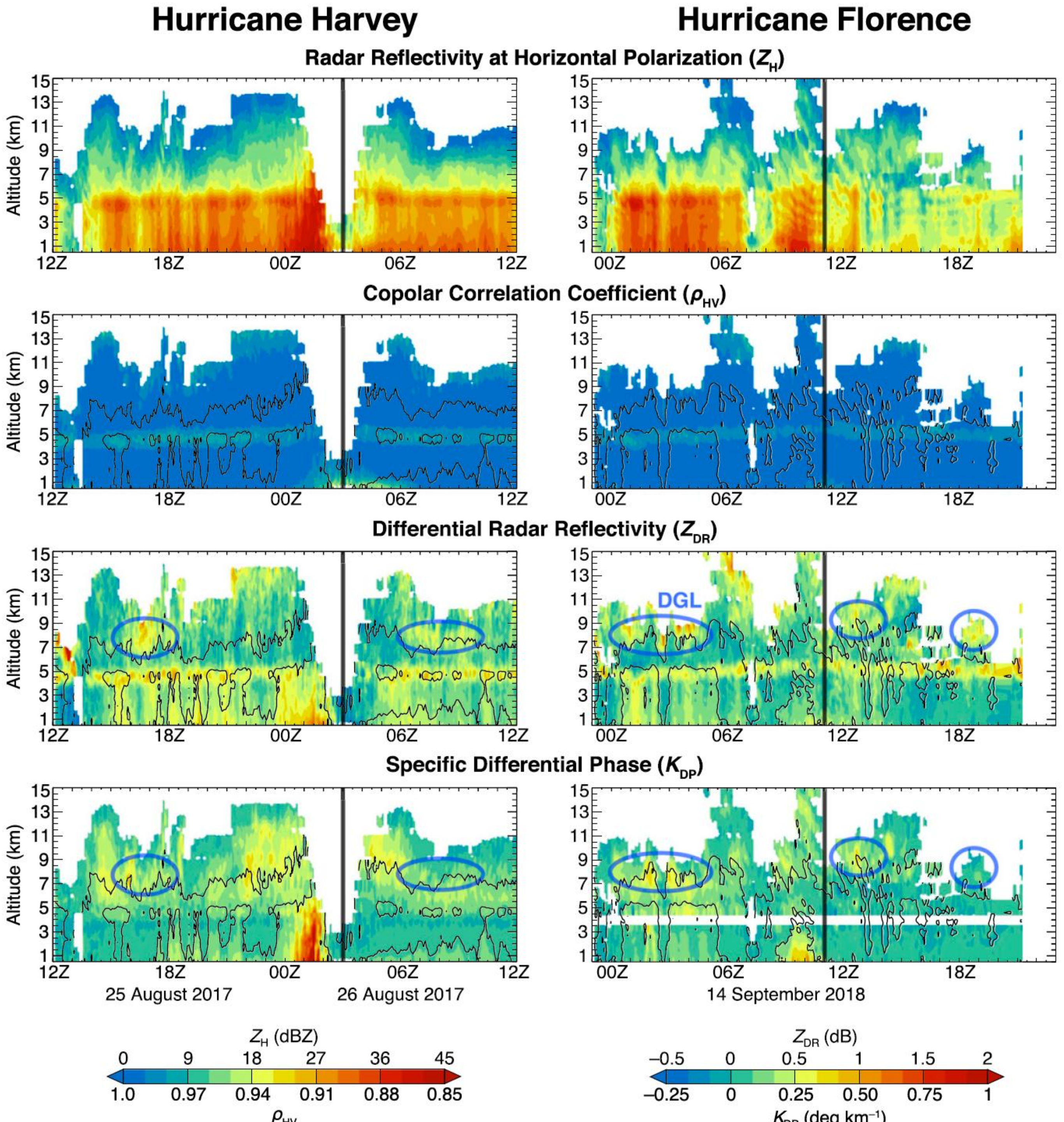

CVPs of polarimetric radar variables for two hurricanes

Homeyer, C., A. Fierro, B. Schenkel, A. Didlake, G. McFarquhar, A. Ryzhkov, J. Basara, A. Murphy, J. Hu, 2021: Polarimetric signatures in landfalling tropical cyclones. *Mon. Wea. Rev.*, **149**, 131 – 154

- Warm rain below the ML
- Upward displacement of the ML near the eyewall
- Abundance of small ice aloft

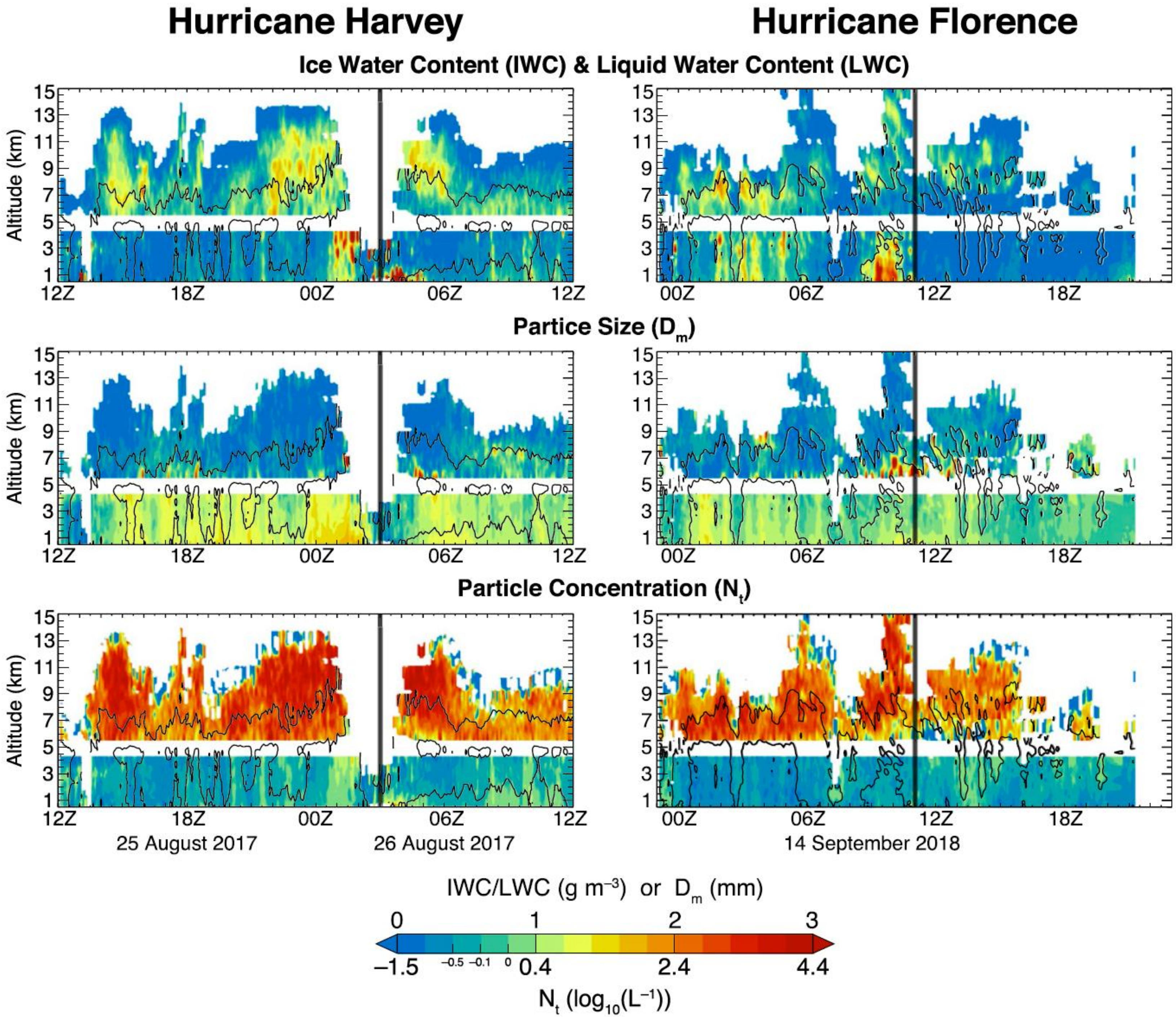

Homeyer et al. 2021

- Very high total number concentration of ice
- Small size of ice

Hurricane Ida track and rain amount

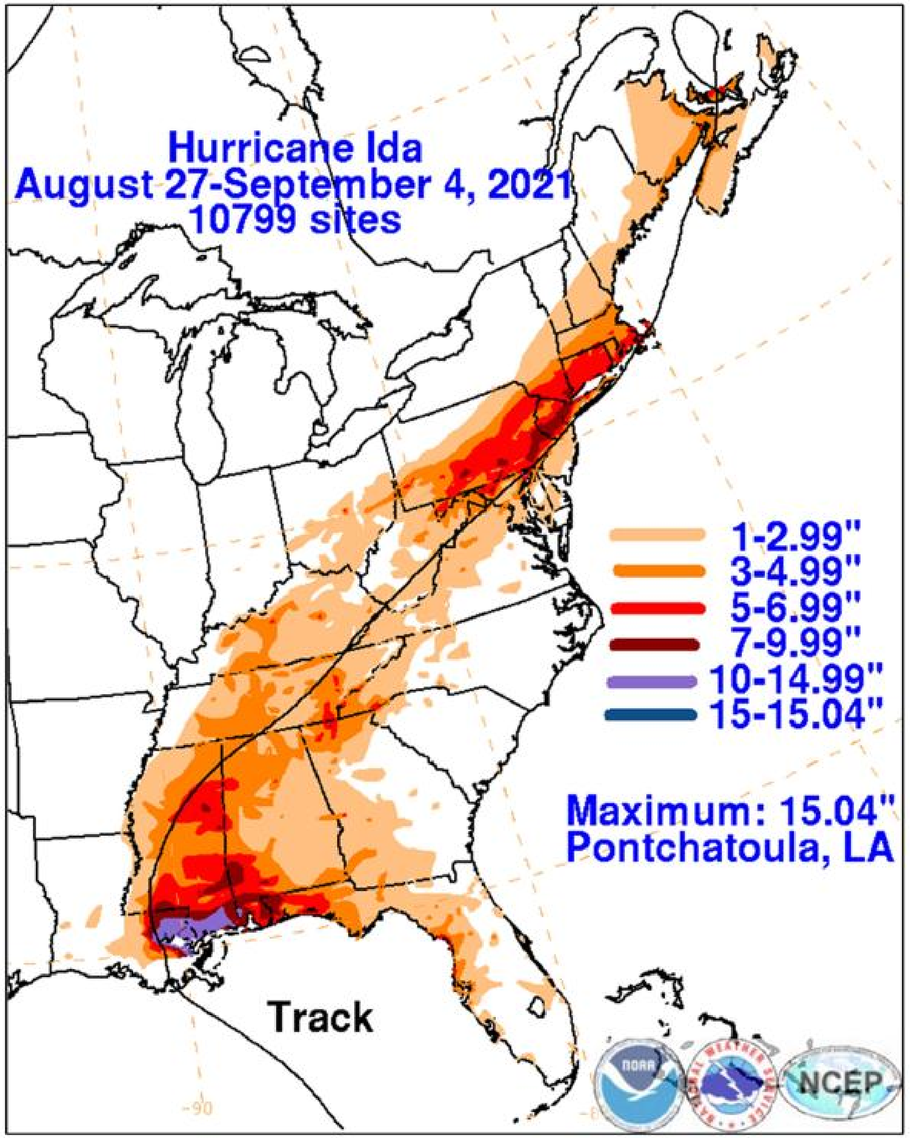

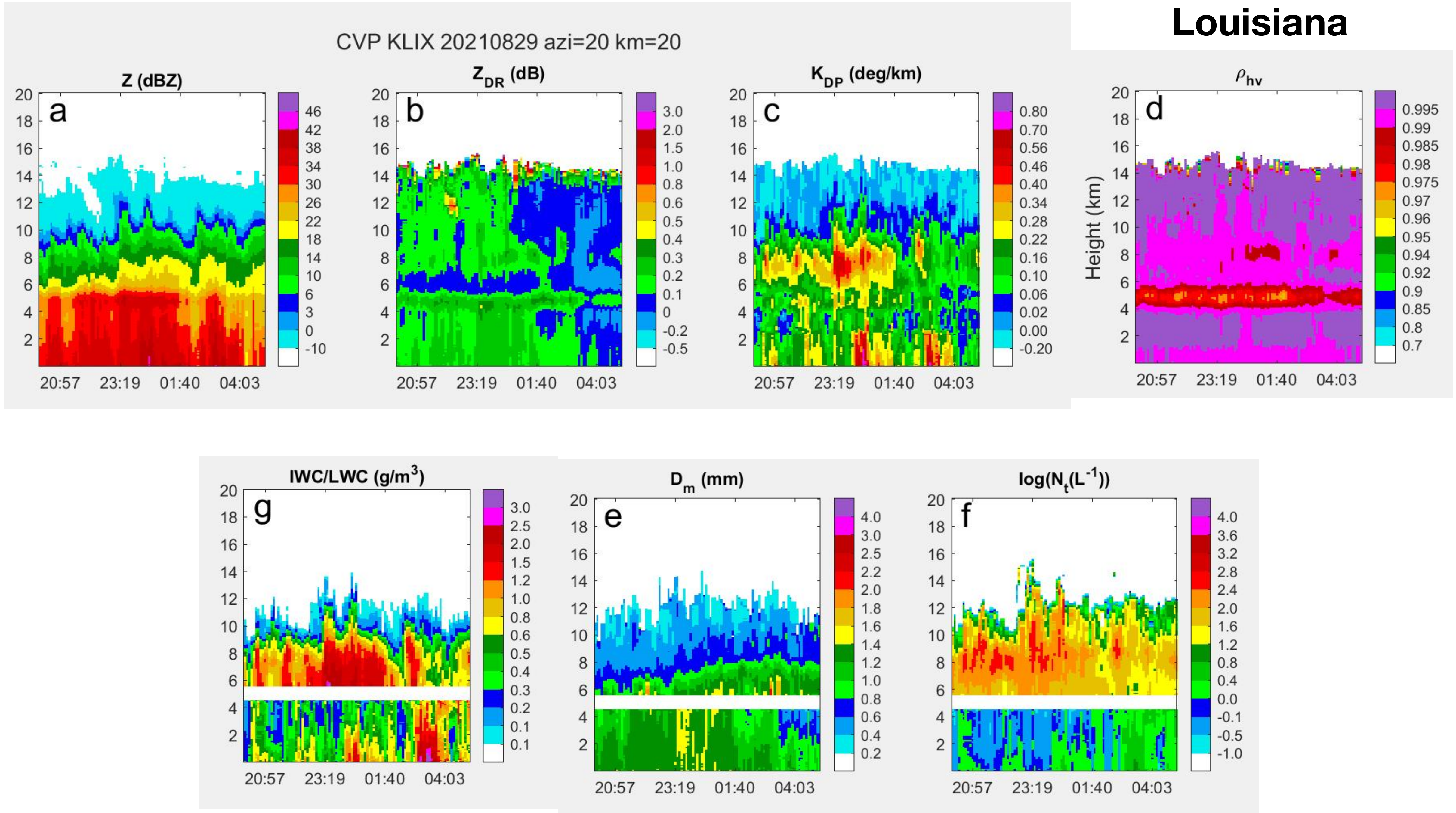

Louisiana
CVP KLIX 20210829 azi=20 km=20
Z (dBZ)
a
46
42
38
34
30
26
22
18
14
10
6
3
0
-10
Z_{DR} (dB)
b
3.0
2.0
1.5
1.0
0.8
0.6
0.5
0.4
0.3
0.2
0.1
0
-0.2
-0.5
K_{DP} (deg/km)
c
0.80
0.70
0.56
0.46
0.40
0.34
0.28
0.22
0.16
0.10
0.06
0.02
0.00
-0.20
ρ_{hv}
d
Height (km)
0.995
0.99
0.985
0.98
0.975
0.97
0.96
0.95
0.94
0.92
0.9
0.85
0.8
0.7
IWC/LWC (g/m^3)
g
3.0
2.5
2.0
1.5
1.2
1.0
0.8
0.6
0.5
0.4
0.3
0.2
0.1
0.1
D_m (mm)
e
4.0
3.0
2.5
2.2
2.0
1.8
1.6
1.4
1.2
1.0
0.8
0.6
0.4
0.2
log(N_t(L^{-1}))
f
4.0
3.6
3.2
2.8
2.4
2.0
1.6
1.2
0.8
0.4
0.0
-0.1
-0.5
-1.0
20
18
16
14
12
10
8
6
4
2
20:57
23:19
01:40
04:03

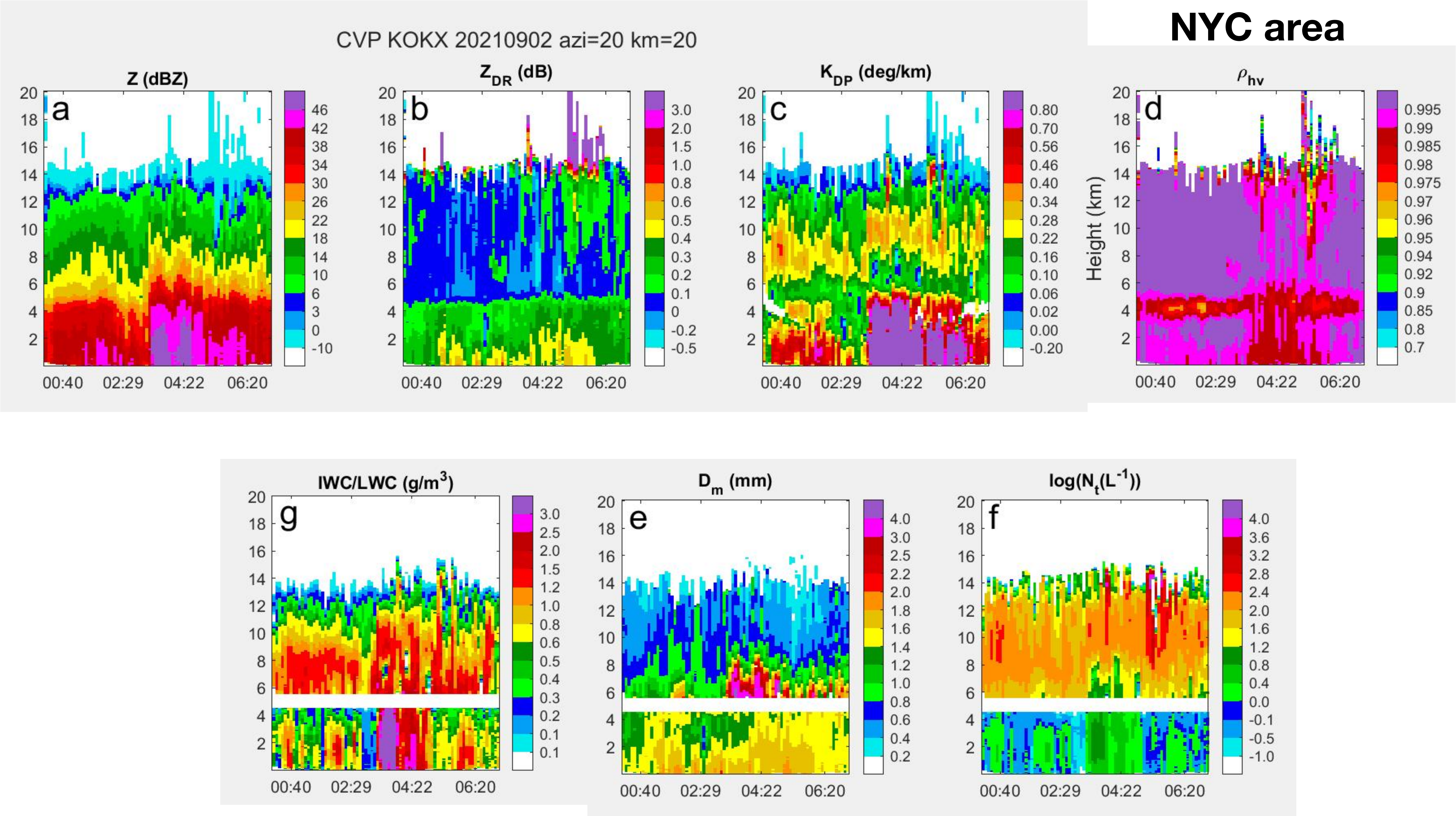
NYC area
CVP KOKX 20210902 azi=20 km=20
Z (dBZ)
Z_{DR} (dB)
K_{DP} (deg/km)
ρ_{hv}
Height (km)
IWC/LWC (g/m^3)
D_m (mm)
log(N_t(L^{-1}))
a
b
c
d
g
e
f
00:40
02:29
04:22
06:20

KBGM WSR-88D radar

Snowstorm Stella

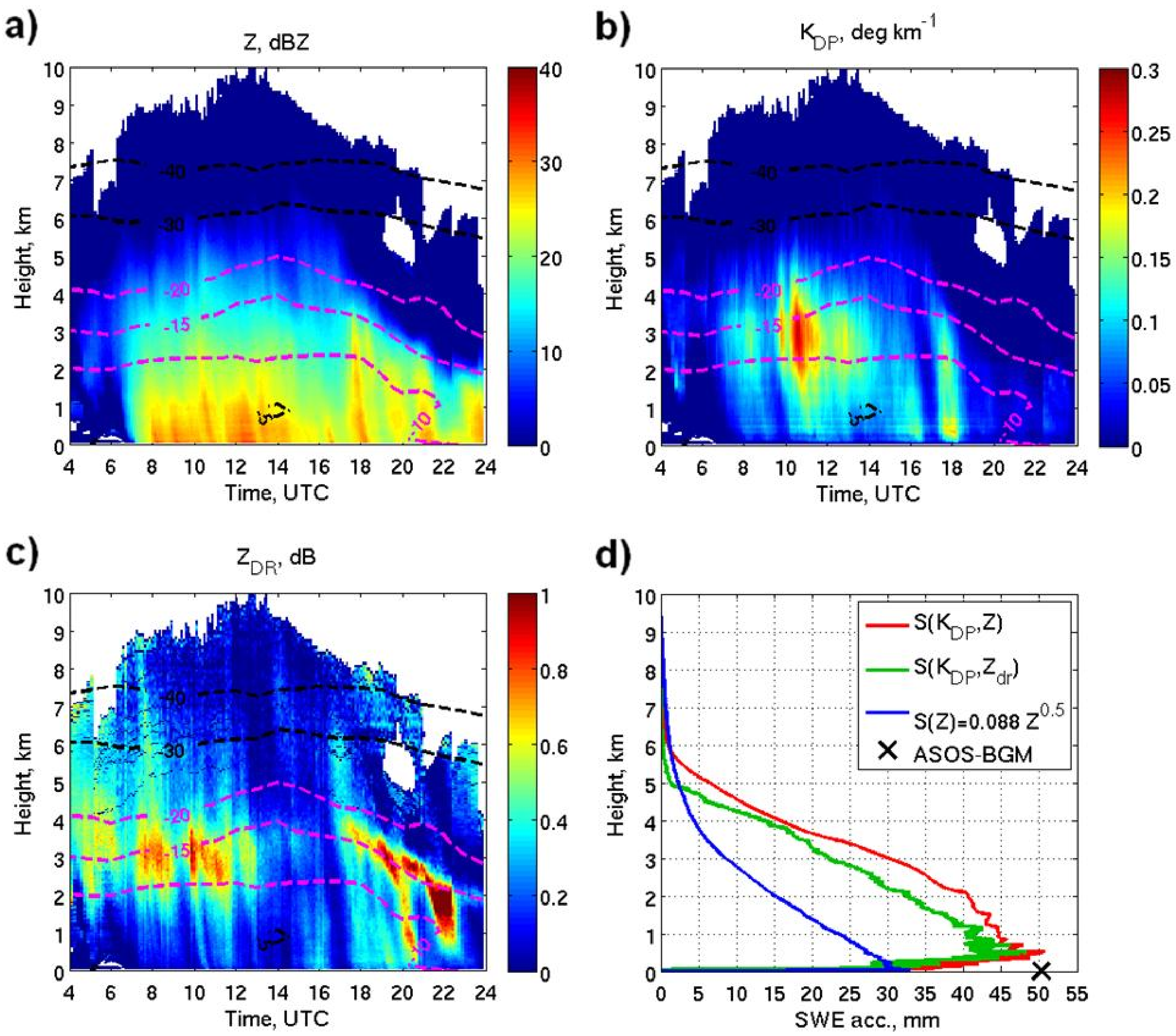

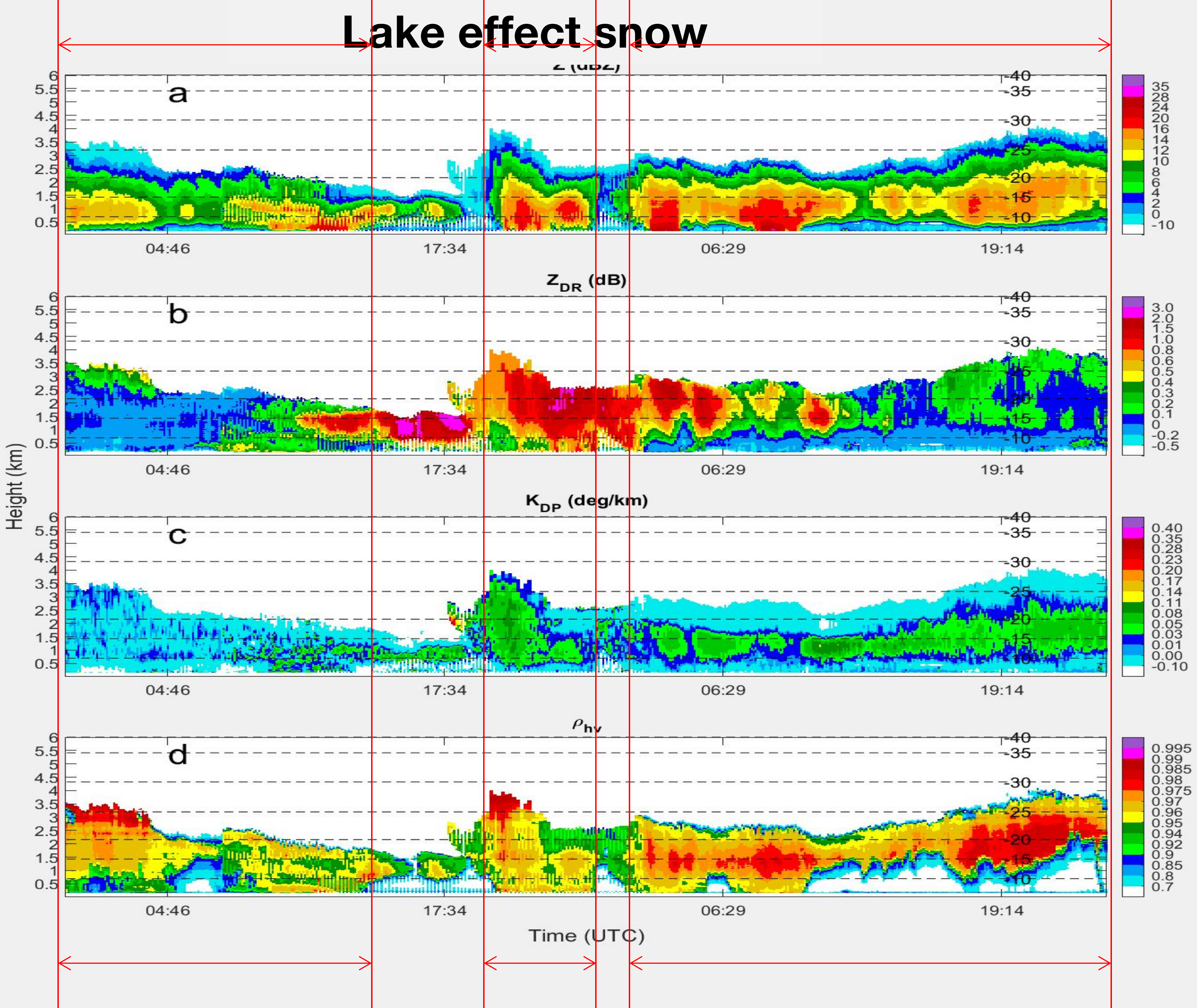

Lake effect snow
Z (dBZ)
Z_DR (dB)
K_DP (deg/km)
ρ_hv
Height (km)
Time (UTC)
04:46
17:34
06:29
19:14
a
b
c
d

Melting and refreezing layers (ML and RL)

S band

Refreezing layer indicates transition from freezing rain to ice pellets

ML

RL

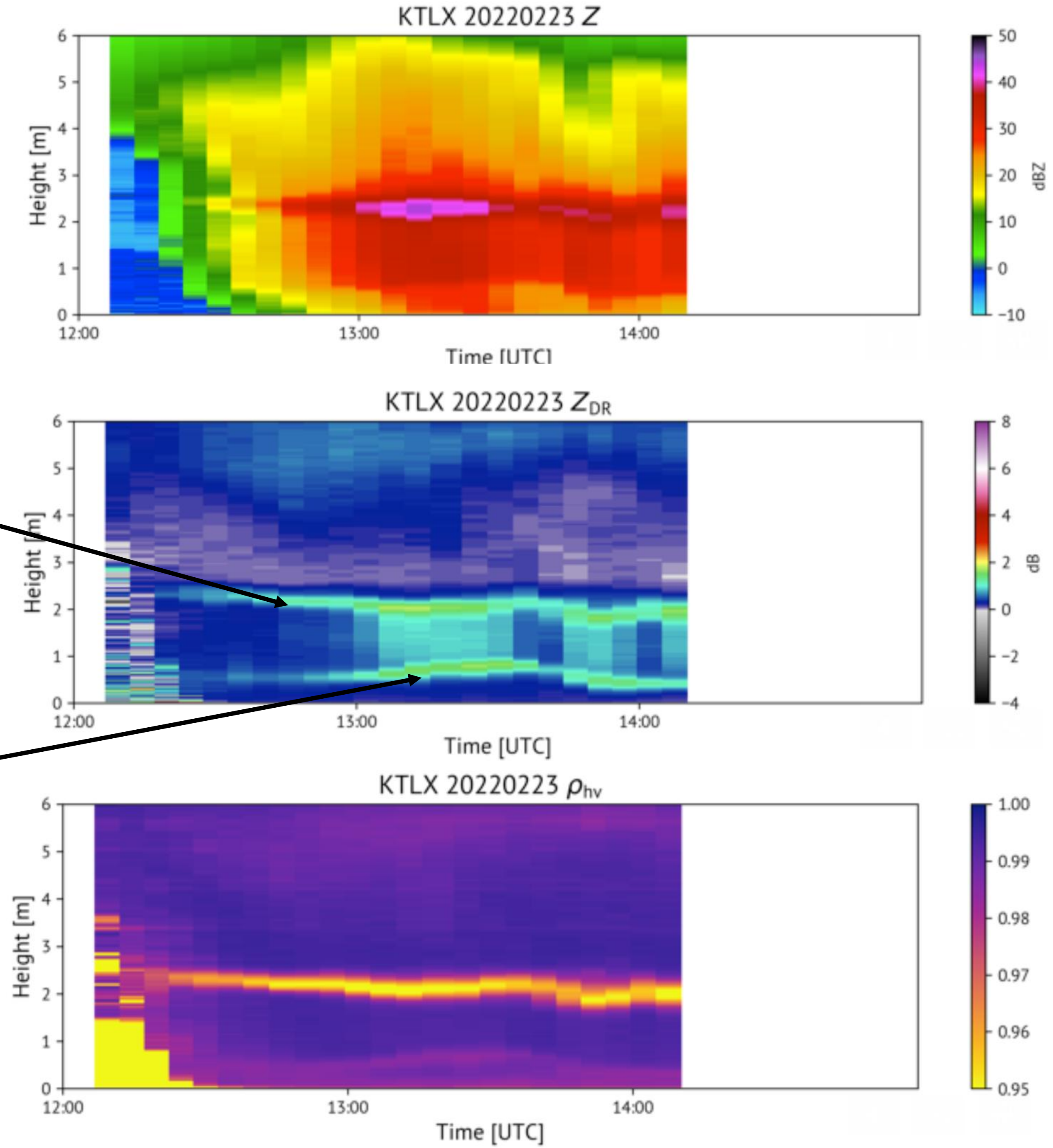

Validation of the ice microphysical retrievals

Ground-based measurements at the Stony Brook University radar facility

Ka band / S band polarimetric radars

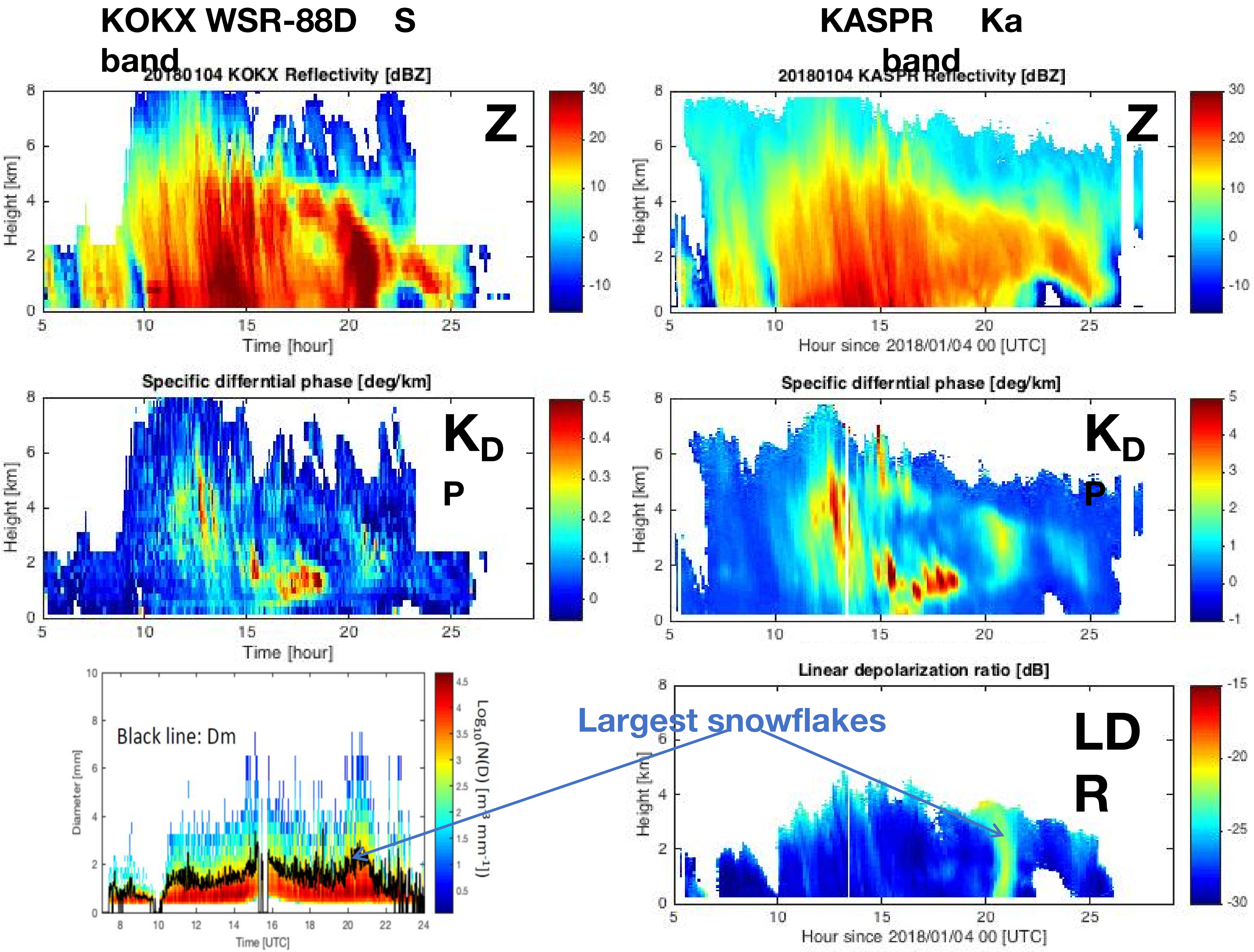

KOKX WSR-88D S band
KASPR Ka band
20180104 KOKX Reflectivity [dBZ]
20180104 KASPR Reflectivity [dBZ]
Z
Height [km]
Time [hour]
Hour since 2018/01/04 00 [UTC]
Specific differntial phase [deg/km]
KDP
Black line: Dm
Diameter [mm]
Time [UTC]
Log10(N(D) [m-3 mm-1])
Linear depolarization ratio [dB]
Largest snowflakes
LDR

Utilization of a short-wavelength radar in combination with a long-wavelength radar

- Polarimetric ice retrieval formulas are valid for Rayleigh scatterers and may not be applicable for snow at Ka band if DWR > > 0 dB

- Because K_{DP} is affected only by Rayleigh-size particles in the spectrum, the product $K_{DP}\lambda$ is almost constant in a wide range of radar frequencies (Ka – S)

- There are two possible ways to make ice retrievals at Ka band

  (1) Utilize $K_{DP}\lambda$ measured at Ka band and Z and Z_{DP} measured at longer wavelength or

  (2) Use Matrosov's formulas to correct Z and Z_{DP} at Ka band

Ka-band QVP and S-band CVP of Z and DWR for two snowstorms

Ka-band Z

S-band Z

DWR

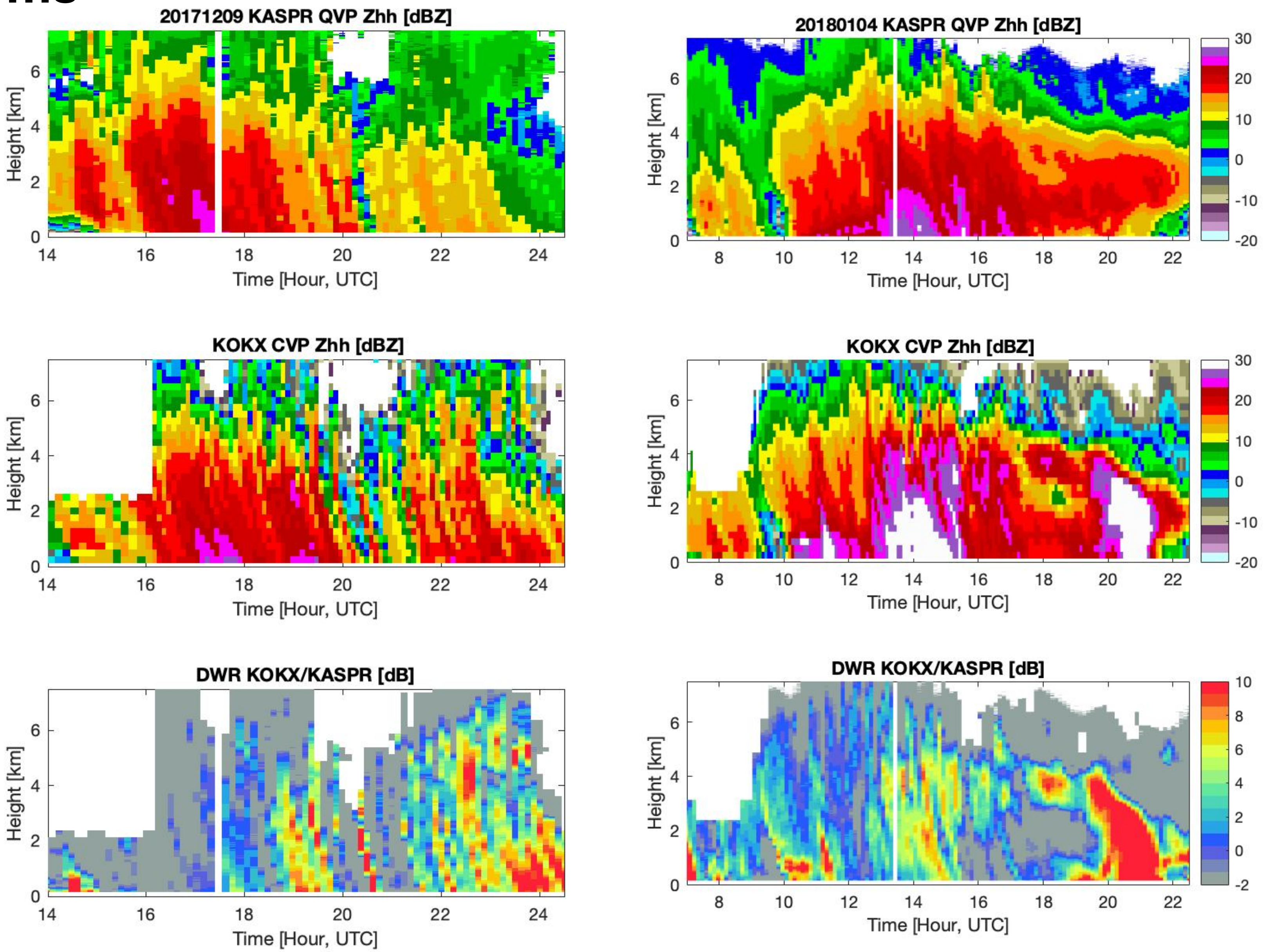

2017/12/09

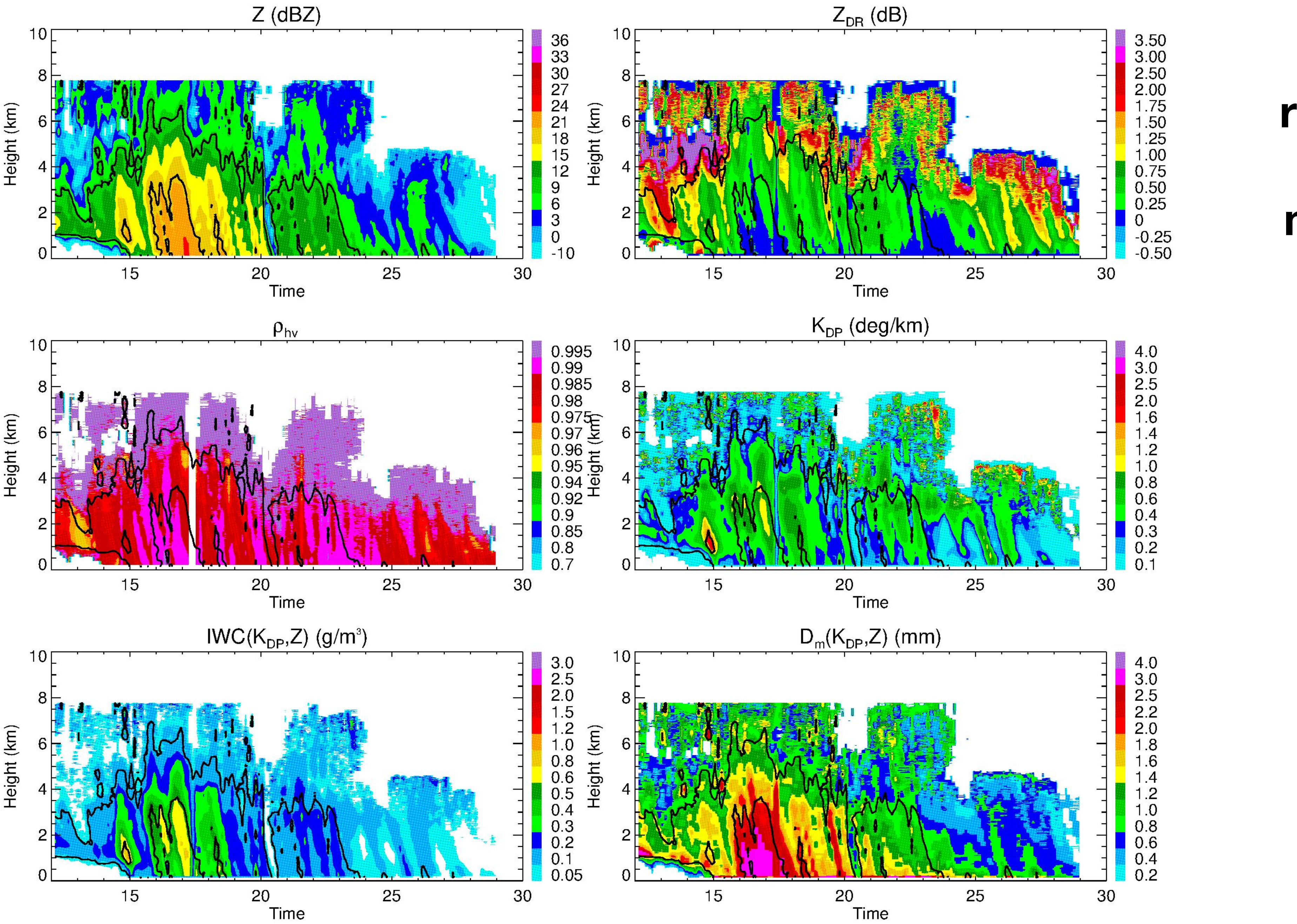

IWC and D_m retrieved from Ka-band measurements

IMPACTS

The **I**nvestigation of **M**icrophysics and **P**recipitation for **A**tlantic **C**oast-**T**hreatening **S**nowstorms

MRMS WSR-88D radar products for the IMPACTS flight on February 7, 2020 (leg 6)

The aircraft flight track is shown by a dashed line

MRMS is the Multi-Radar Multi-Sensor integration platform

Composite radar reflectivity

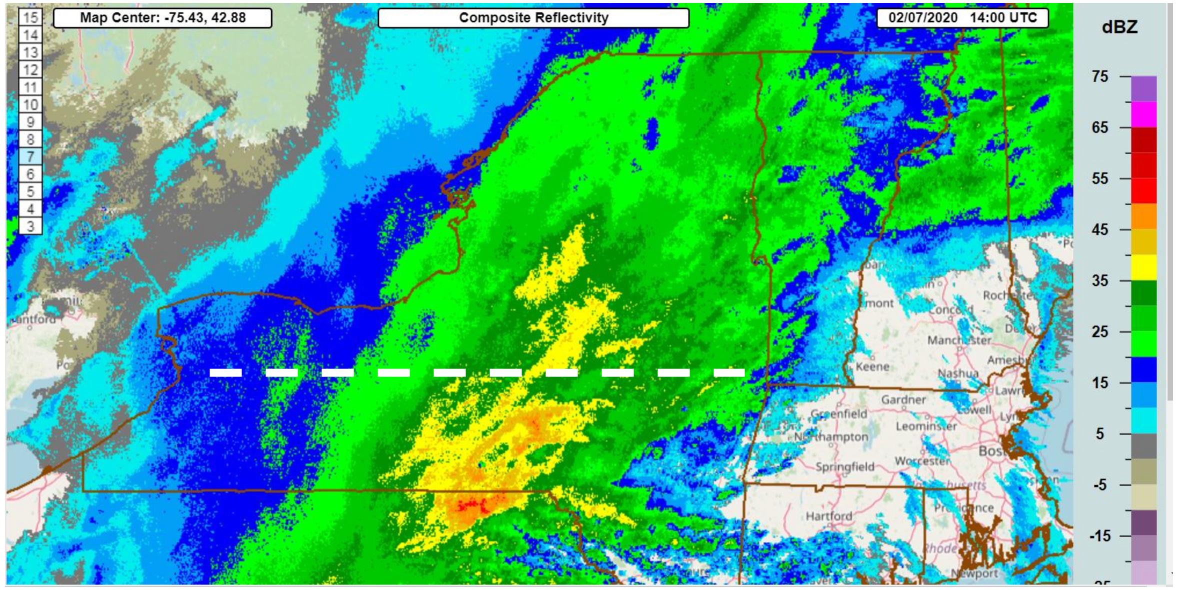

Z_{DR} at the 2 km altitude

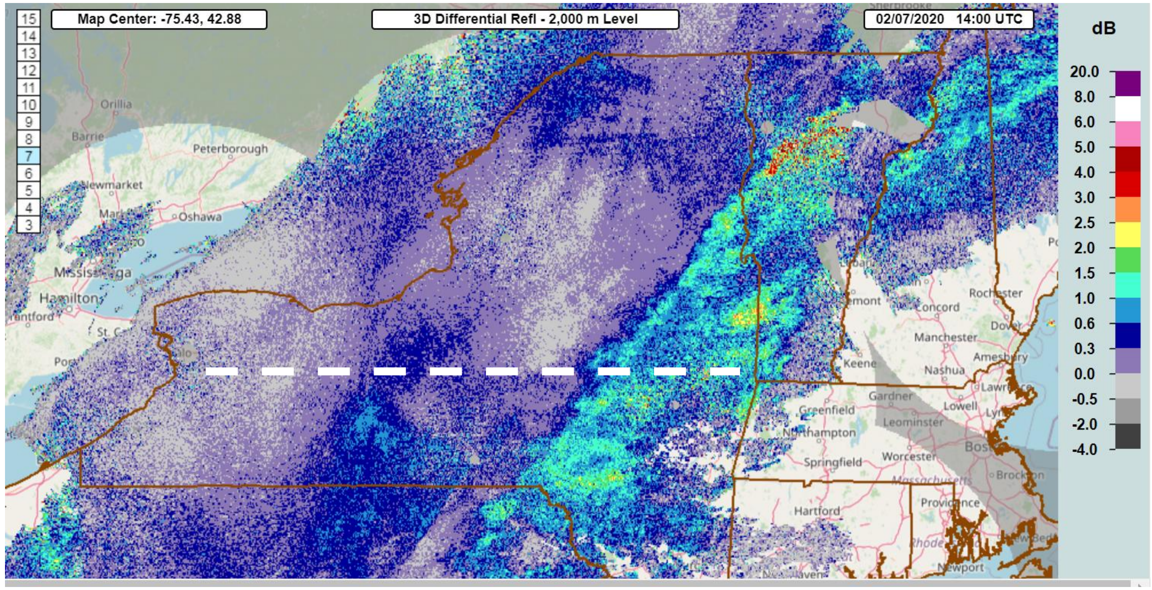

CC at the 2 km altitude

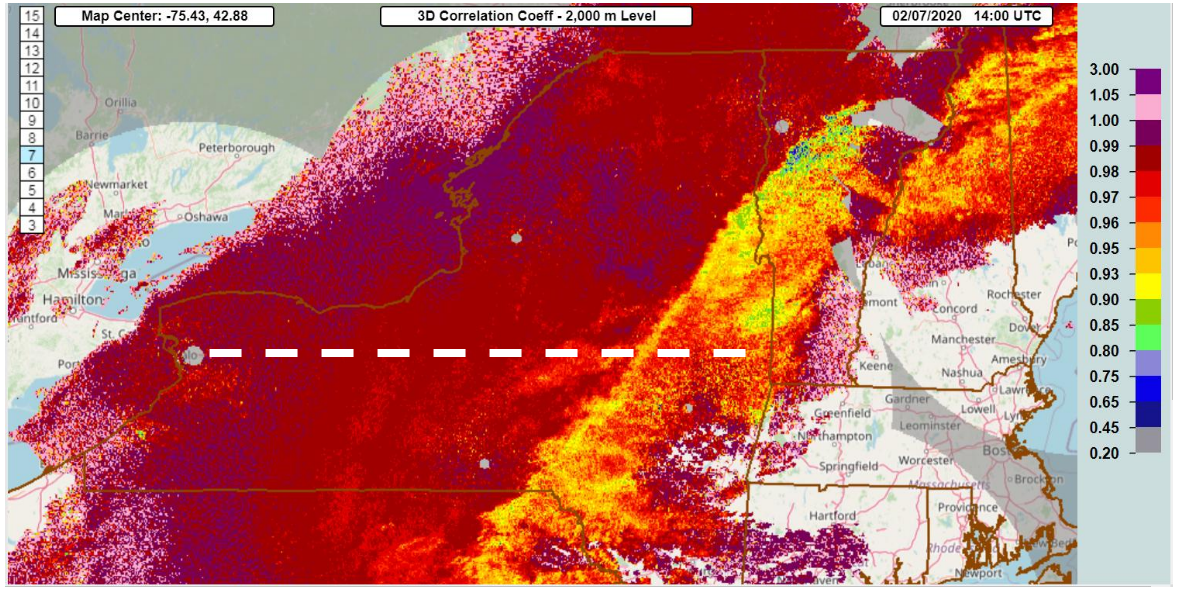

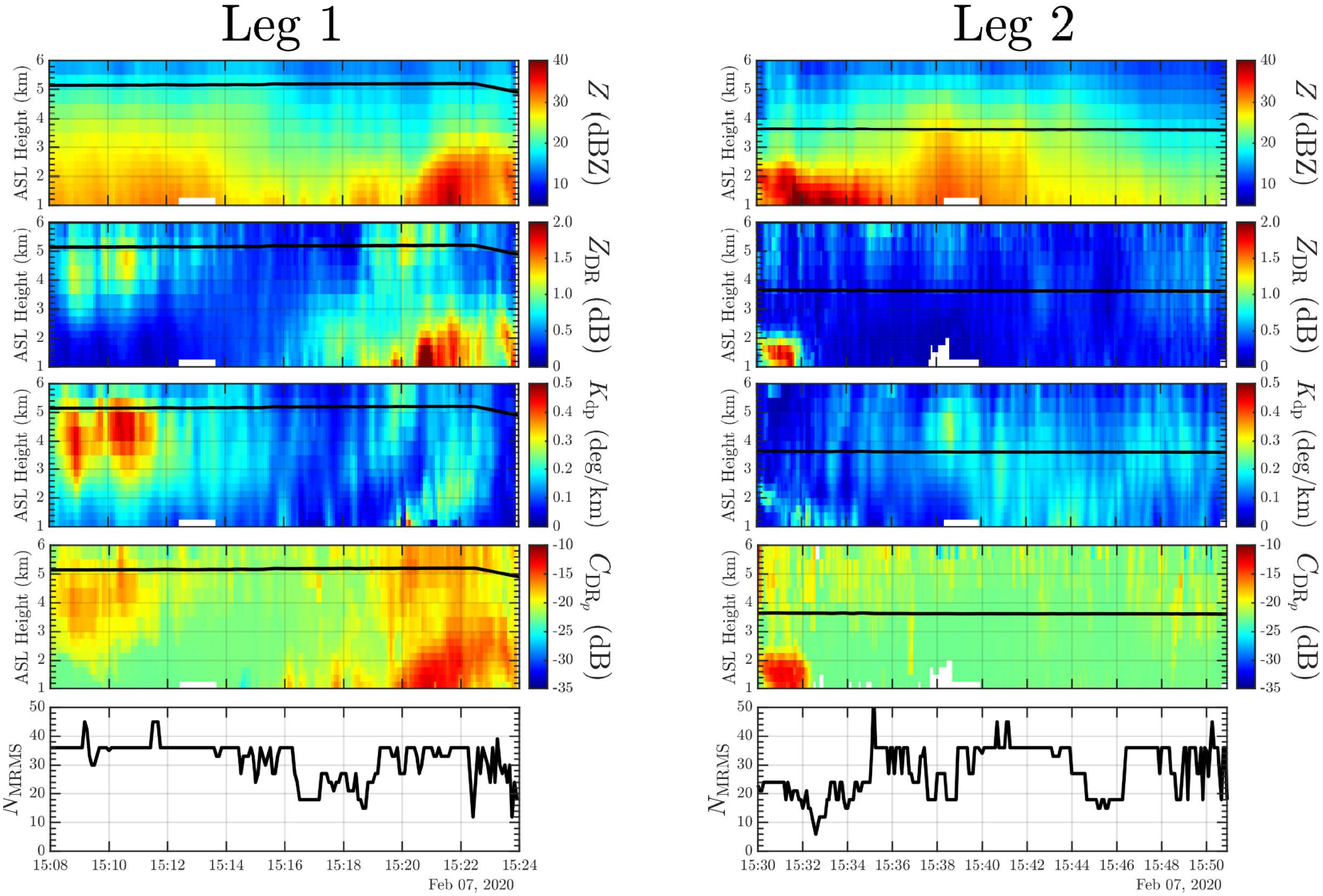

Leg 1
Leg 2
ASL Height (km)
Z (dBZ)
Z_DR (dB)
K_dp (deg/km)
C_DR_p (dB)
N_MRMS
15:08 15:10 15:12 15:14 15:16 15:18 15:20 15:22 15:24
15:30 15:32 15:34 15:36 15:38 15:40 15:42 15:44 15:46 15:48 15:50
Feb 07, 2020

Dunnavan et al. 2022

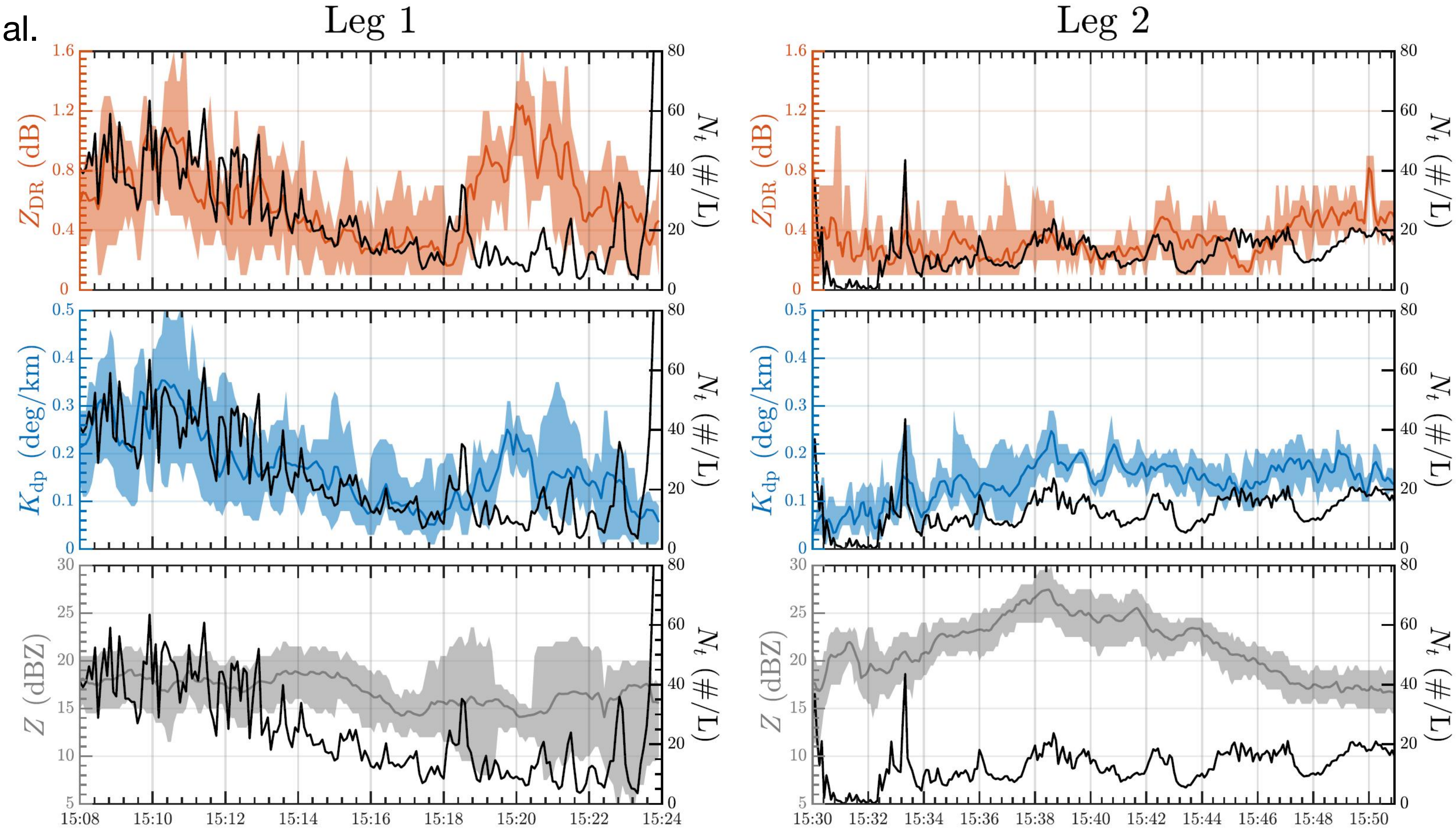

- K_{DP} exhibits the best correlation with the total number concentration N_t of ice
- Z does not correlate with N_t at all

Varcie et al. 2022

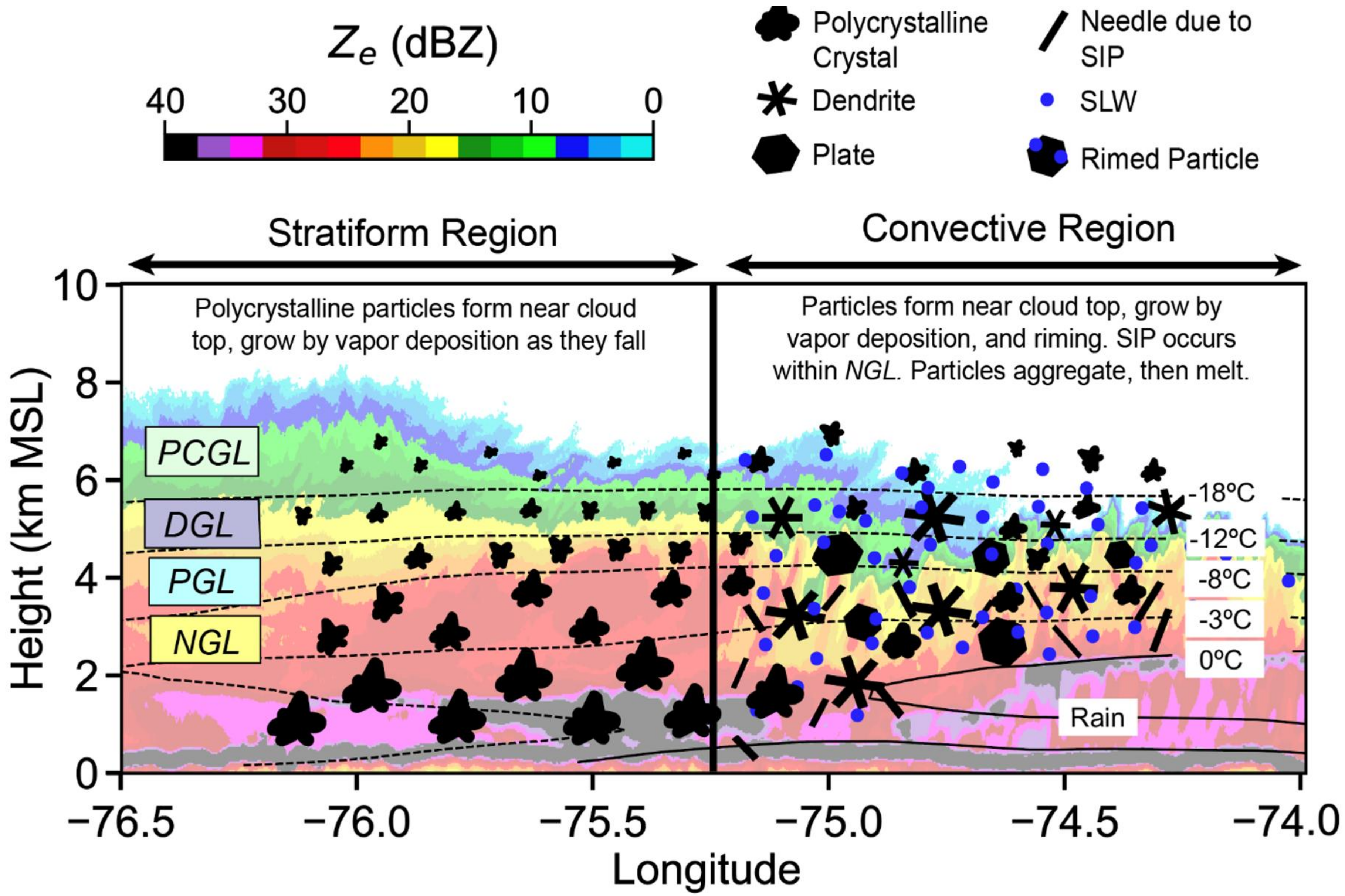

Varcie et al. 2022

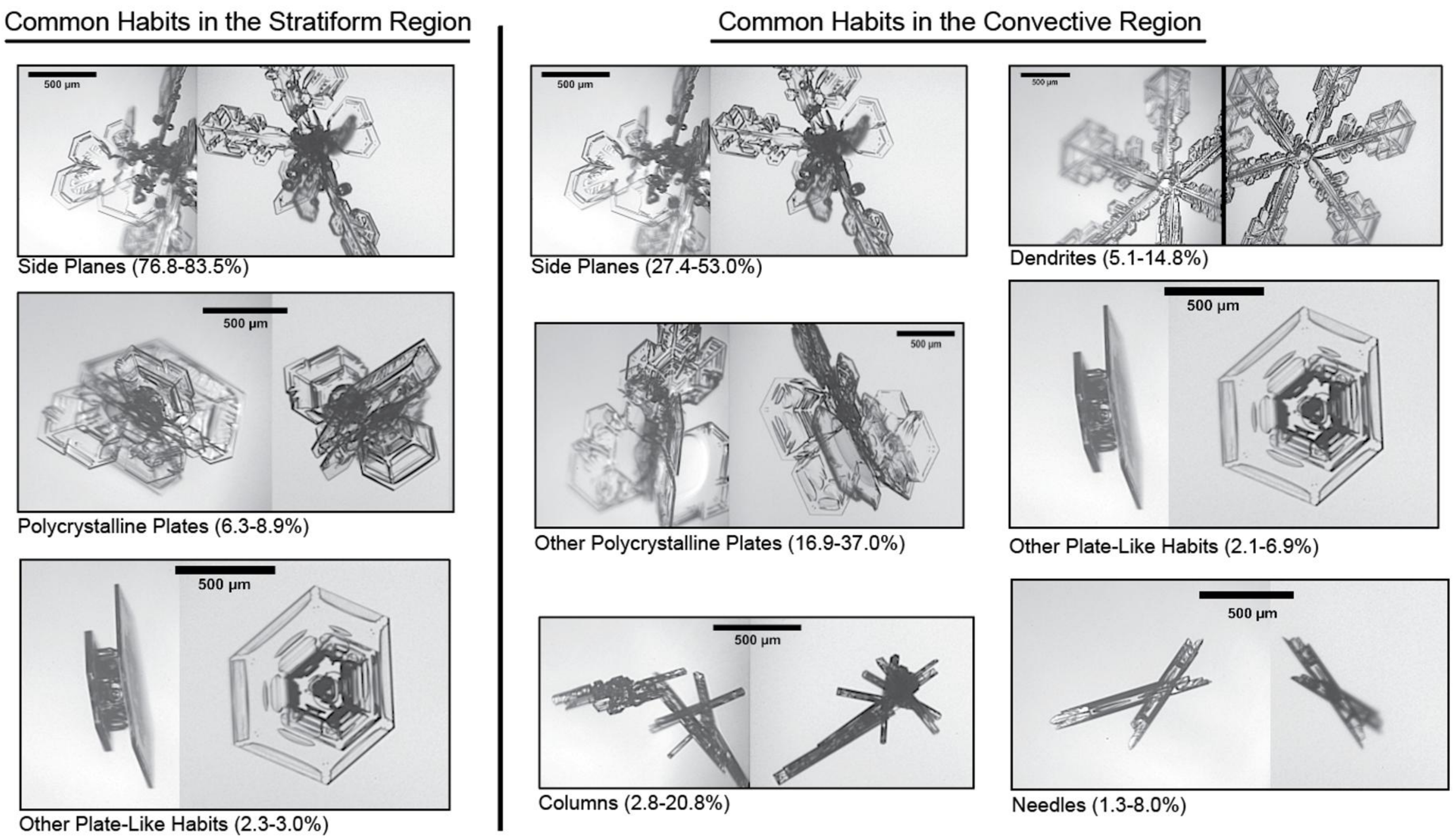

Comparison with in situ aircraft observations in ice Preliminary results

- Polarimetric microphysical retrievals have been evaluated using in situ aircraft observations during 5 field campaigns so far

(1) HAIC – HIWC	French Guiana	Nguyen et al. (2019)
(2) MC3E	Oklahoma	Murphy et al. (2020)
(3) IMPACTS	US Northeast	Dunnavan et al. (2022)
(4) OLYMPEX	US Northwest	Blanke et al. (2022) ?
(5) ICICLE	US Midwest	?

- The results are generally encouraging
- The best results have been obtained with dedicated X-band polarimetric radars

Climatology

Dataset includes 34 warm-season storms (13 continental MCSs, 10 maritime MCSs, and 11 land-falling hurricanes) and 22 snowstorms (synoptic and lake effect) observed with the WSR-88D radars

Separate statistics have been obtained: (a) “background” and (b) High Ice Water Content (HIWC)

RD-QVPs and CVPs have been used to retrieve vertical profiles of polarimetric radar variables and microphysical parameters (IWC / LWC, D_m, and N_t)

Hu, J., and A. Ryzhkov, 2022: Climatology of the vertical profiles of polarimetric radar variables and retrieved microphysical parameters in continental / tropical MCSs and landfalling hurricanes. *J. Geophys. Res. Atmos.*, 127, e2021JD035498.

Median vertical profiles. "Background" statistics.

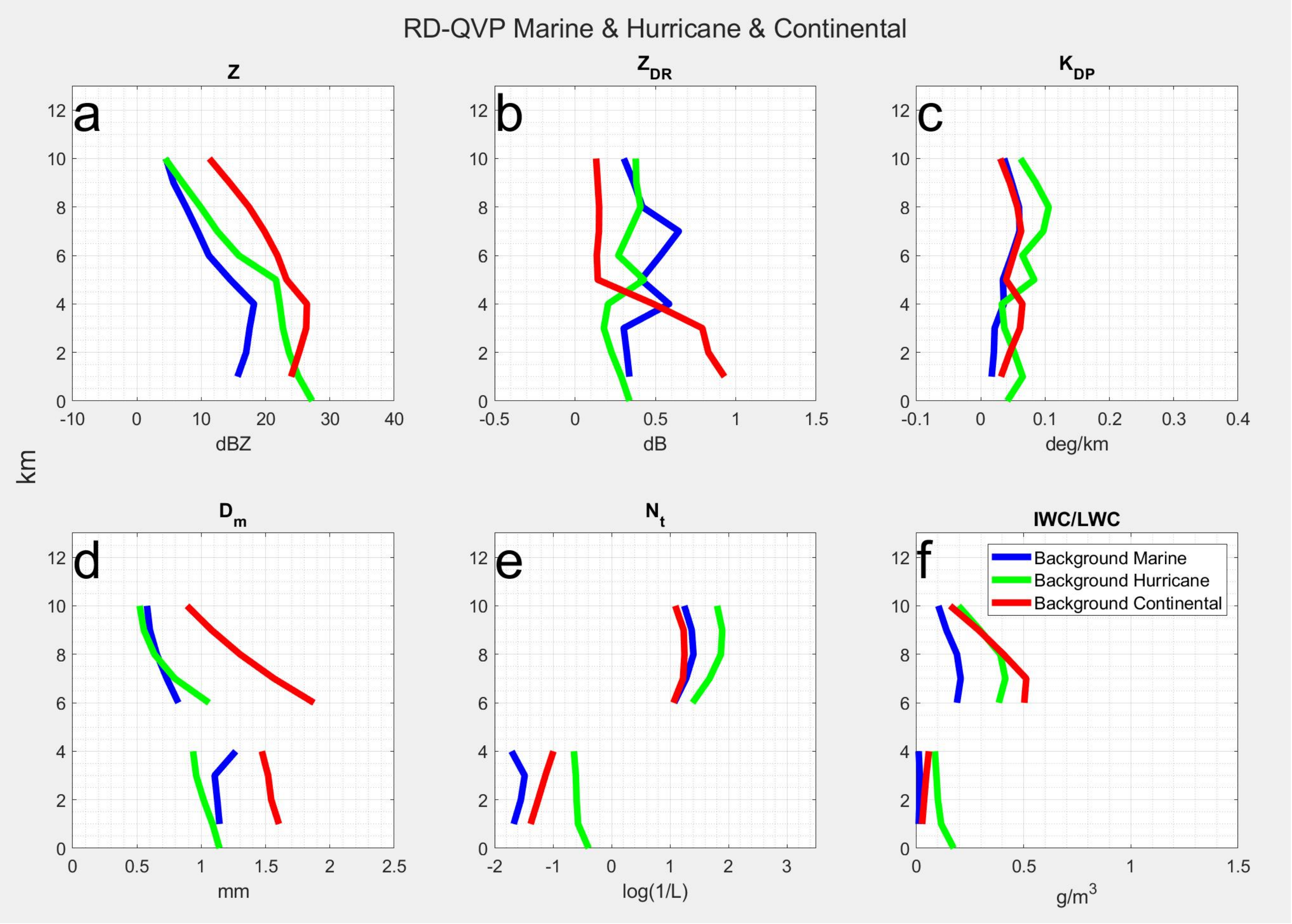

Ice particles in continental MCSs have larger size and lower concentration compared to the maritime storms

Median vertical profiles. HIWC statistics.

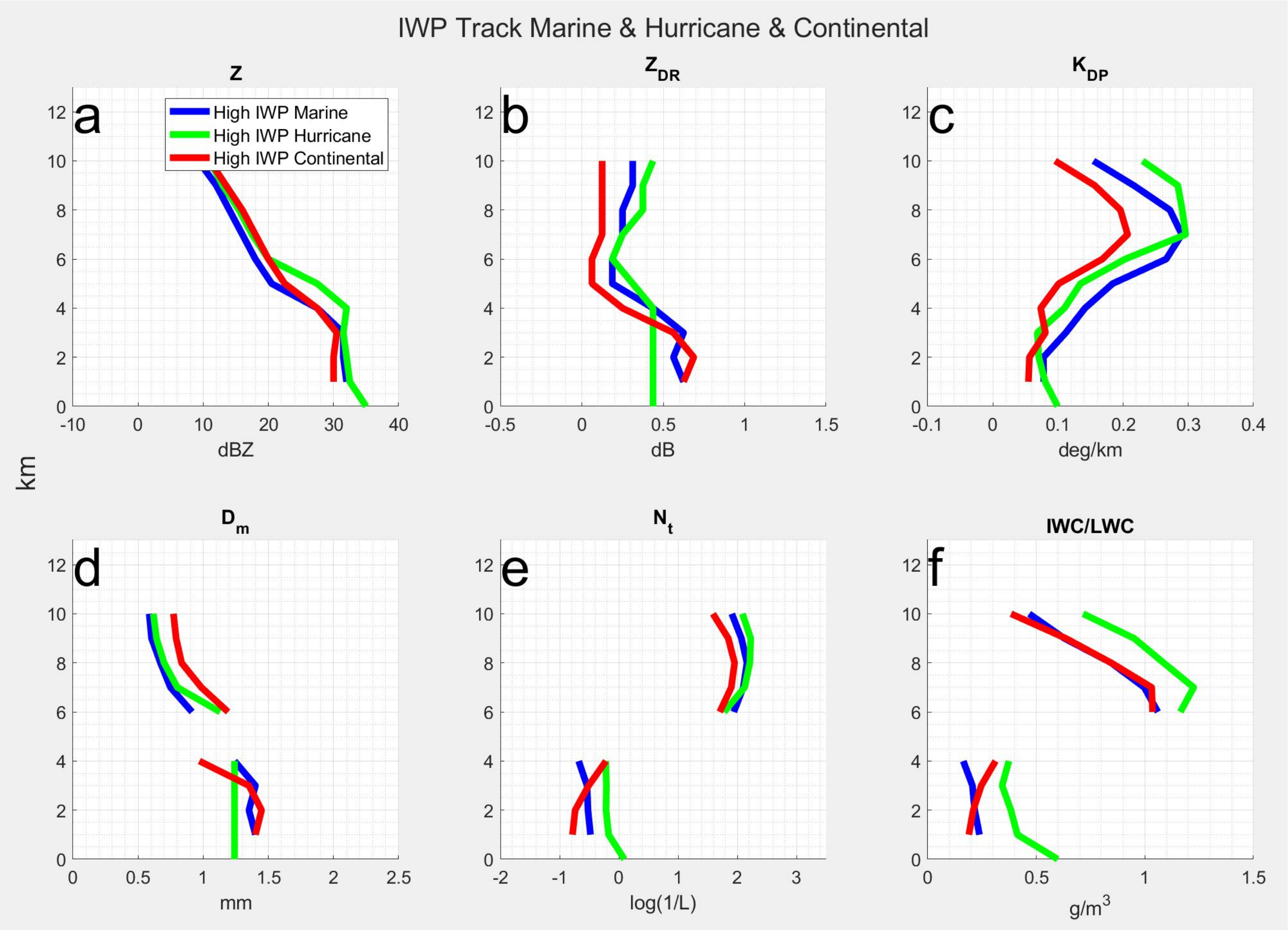

High ice water content in the HIWC areas is primarily caused by a strong jump in a number concentration of ice particles rather than the increase of their size compared to the “background” environment

Snowstorms (synoptic). “Background” statistics

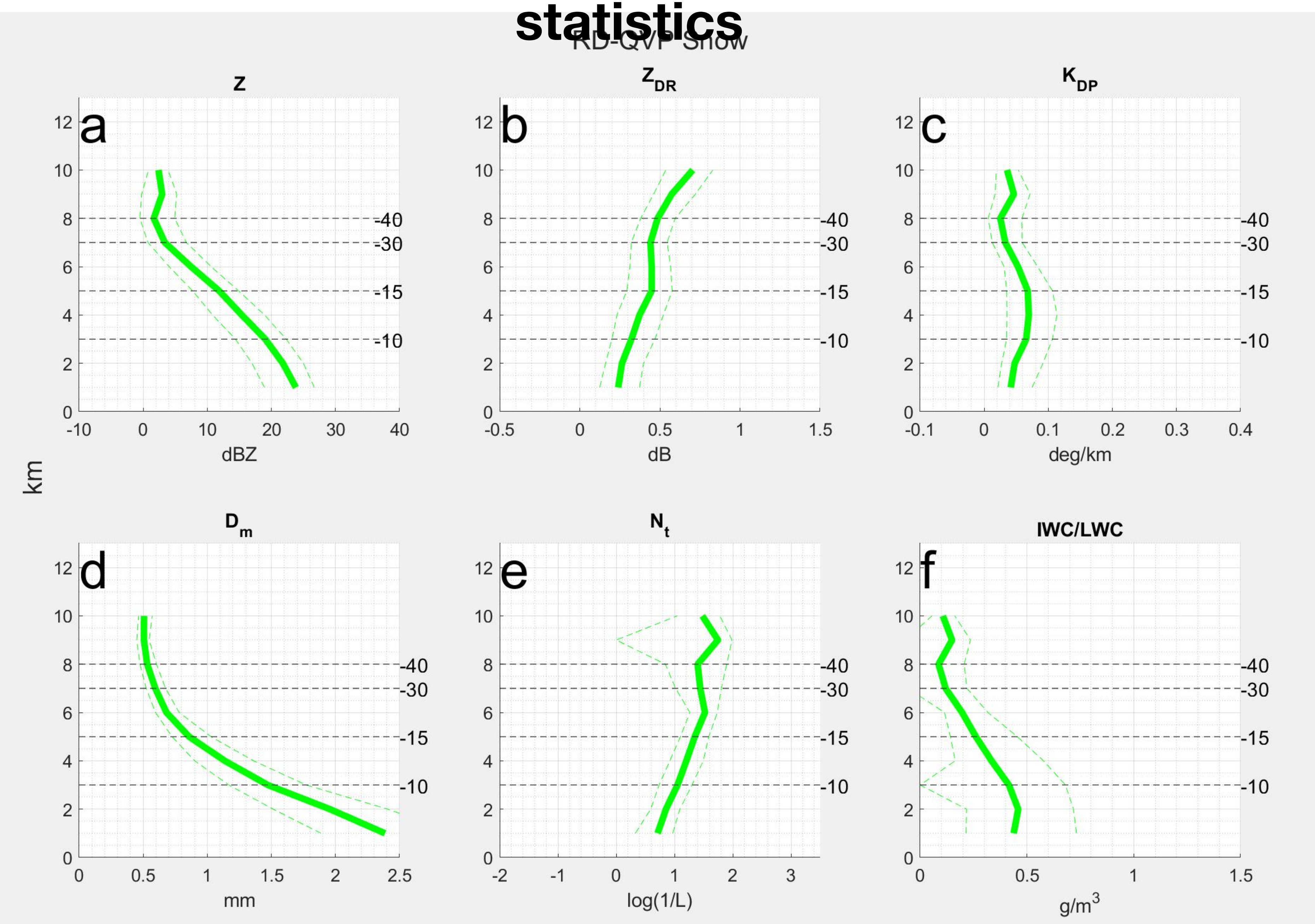

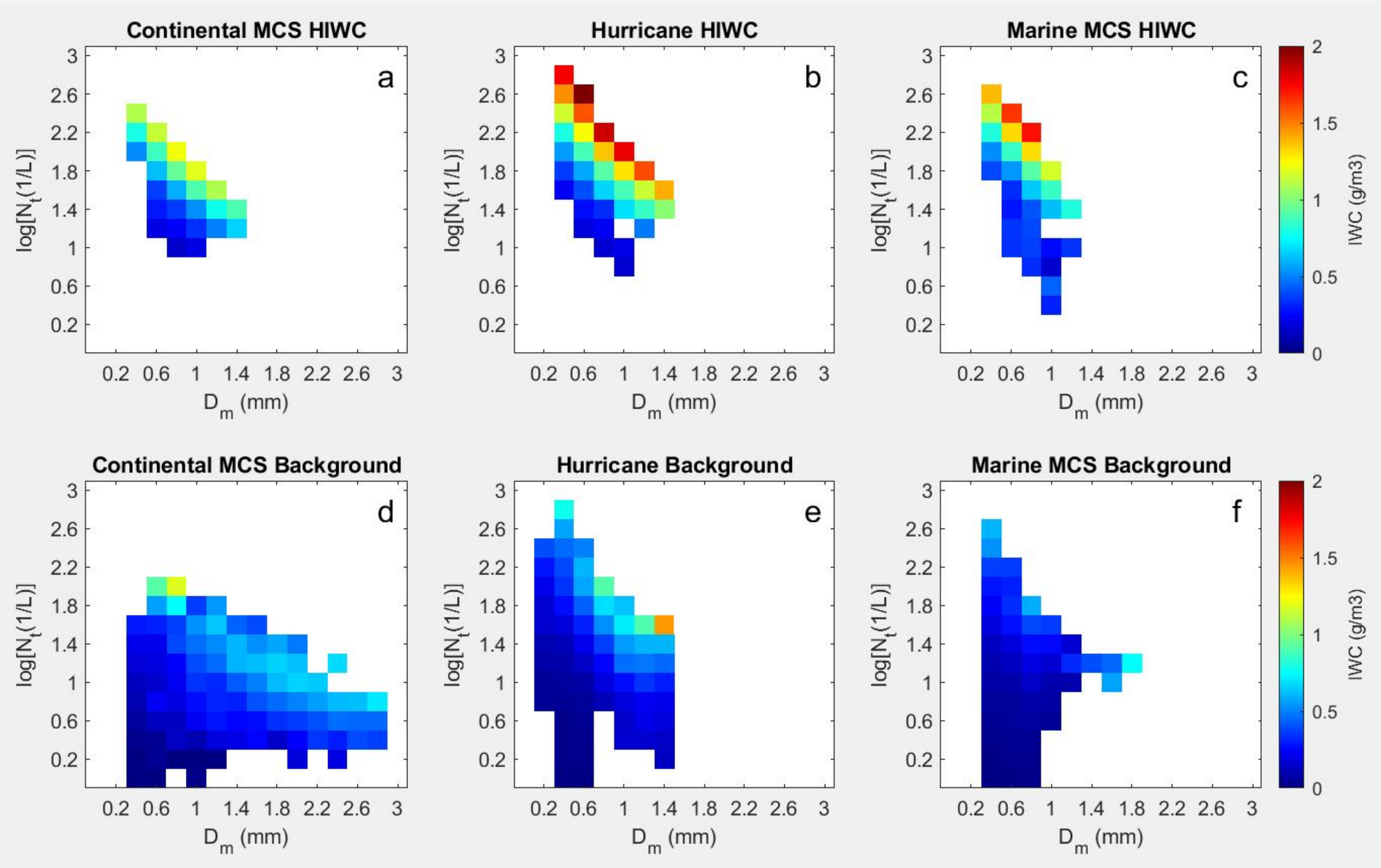

The highest median values of IWC approaching 1.5 – 2 g m^{-3} are observed in the hurricanes and marine MCSs and these are primarily associated with the highest total number concentrations of ice N_t and smallest sizes of ice particle D_m (panels b and c). The continental MCSs reveal quite different pattern with noticeably lower median values of IWC even for HIWC cases (panels a and d).

Possible origins of high ice number concentration

- Intense homogeneous nucleation of liquid droplets at T < -37°C

- Secondary ice production (SIP) due to Hallett-Mossop process

- SIP caused by dendrite – graupel collisions in convective updrafts (deep continental convection) – V. Phillips at al.

- SIP caused by shattering of freezing raindrops lofted in convective updrafts (tropical storms) – A. Khain

- SIP caused by spontaneous breakup of dendrites in the dendritic growth layer – Korolev et al.

- SIP caused by sublimation of ice crystals

Maritime MCS on 2020/05/14 observed by the WSR-88D radar at Key West

Radar reflectivity at 8.5 km

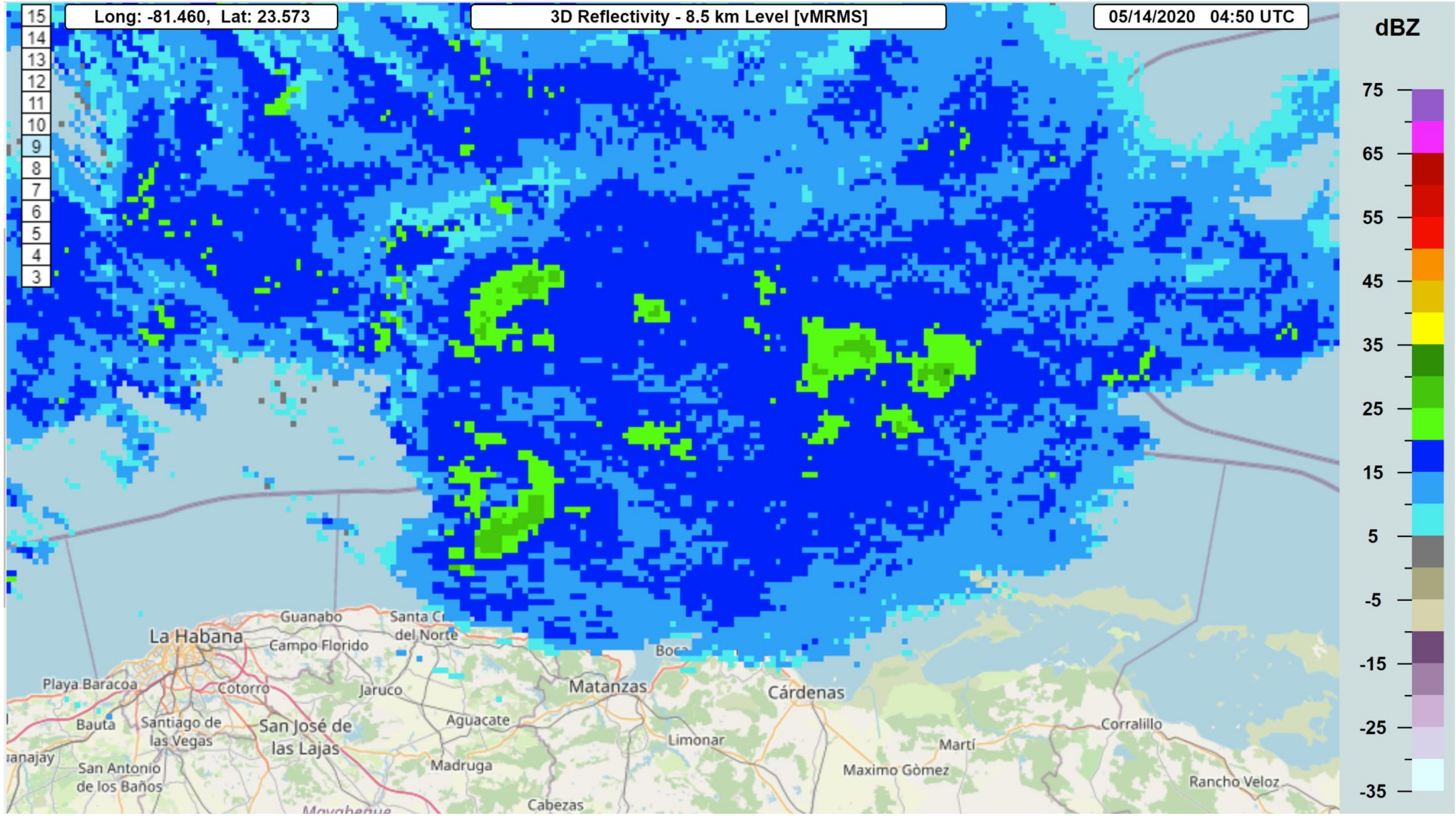

Specific differential phase at 8.5 km

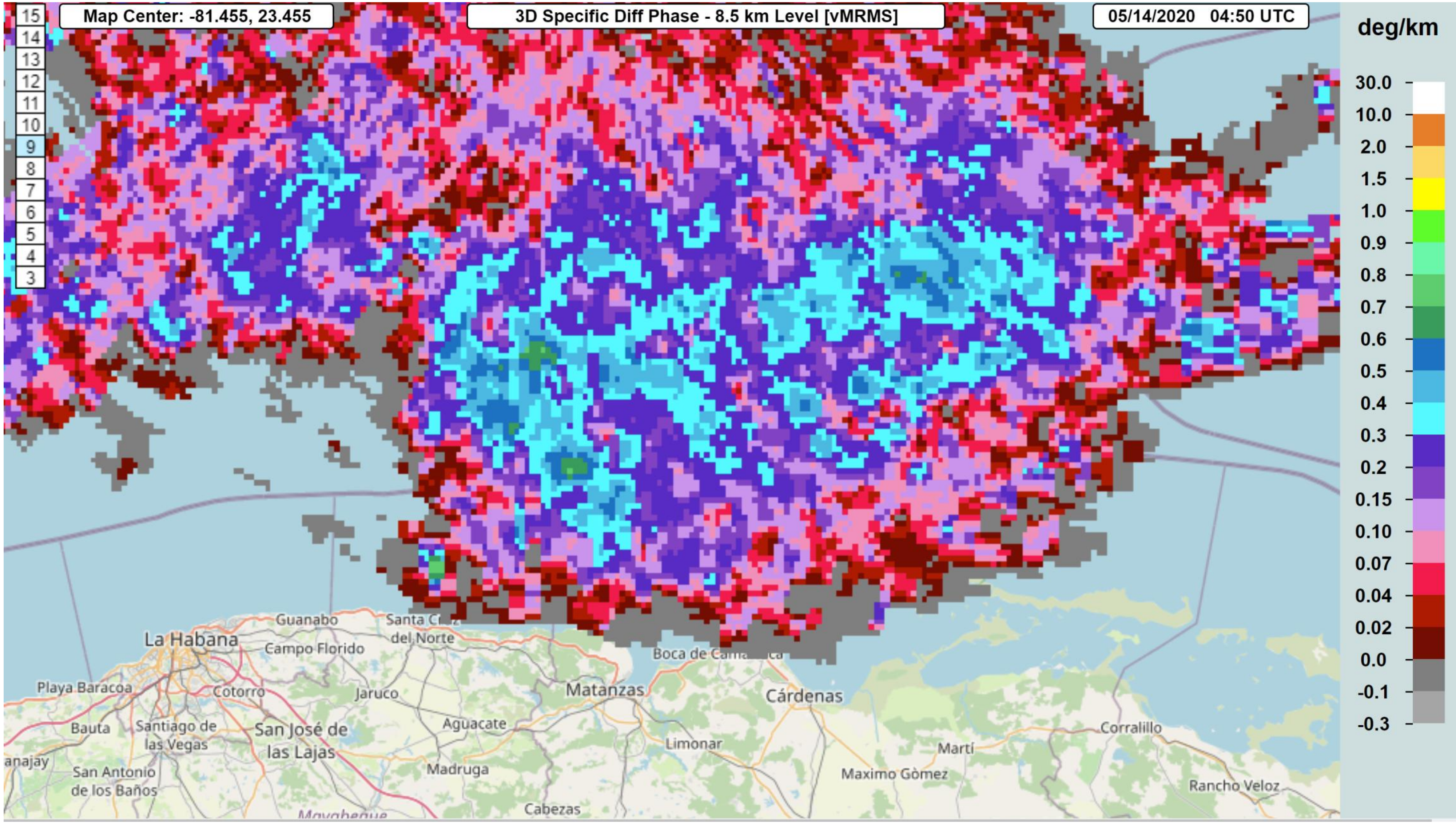

2021-09-30 17:49:08 - RHI at Az = 57

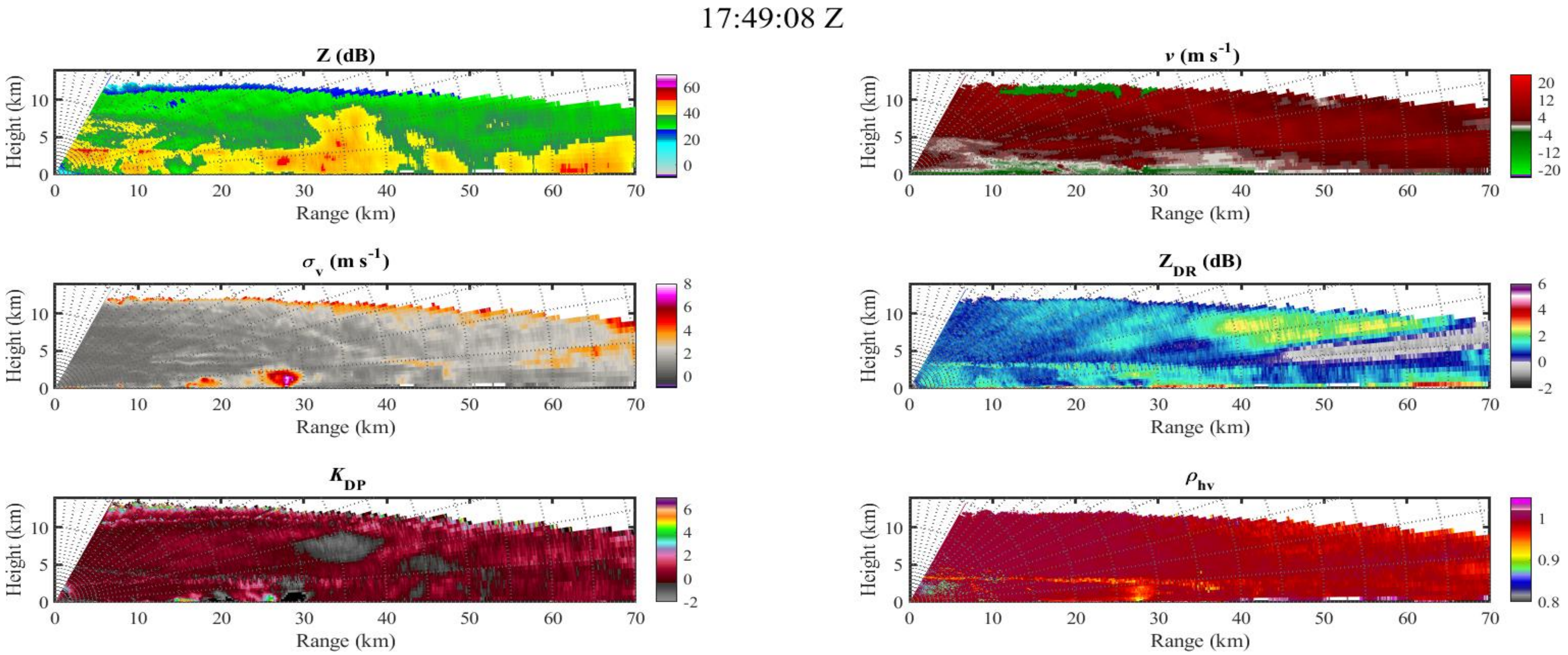

2021-09-30 17:49:13 - RHI at Az = 57

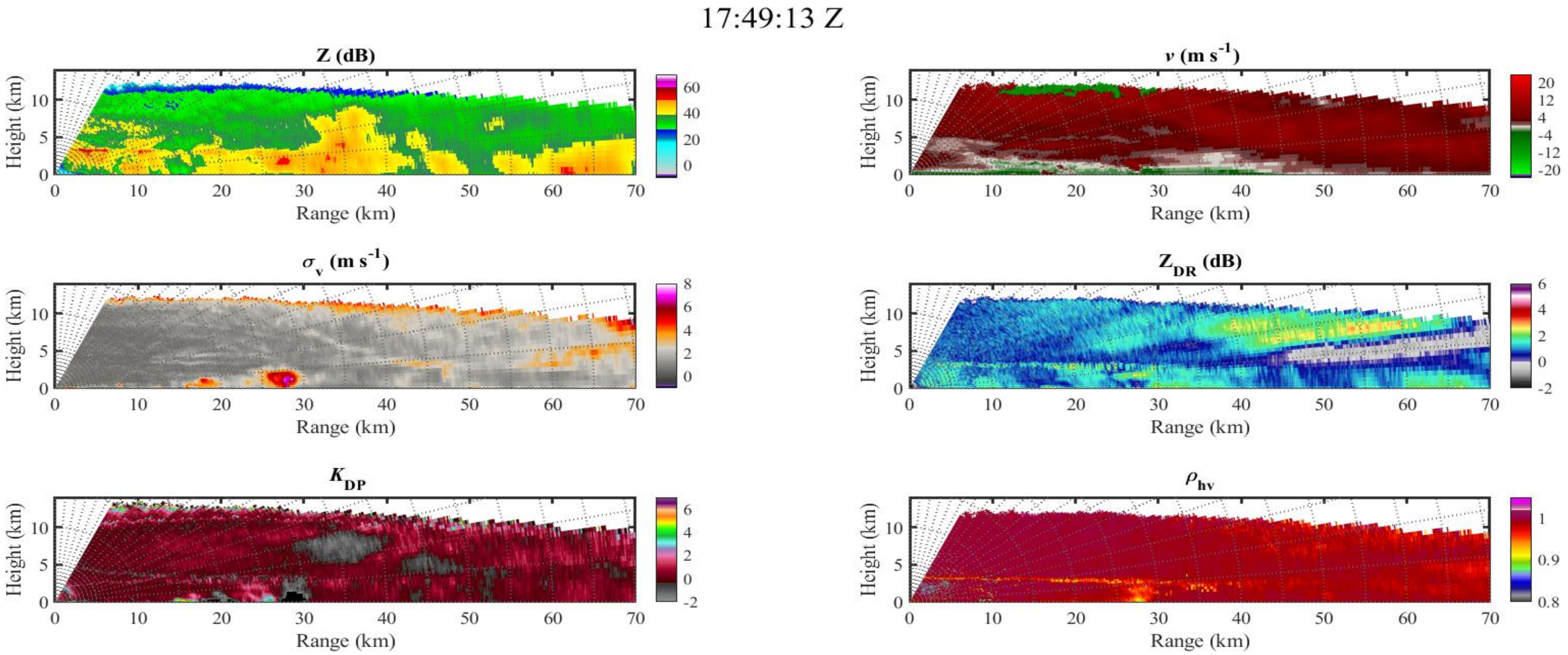

2021-09-30 17:49:17 - RHI at Az = 57

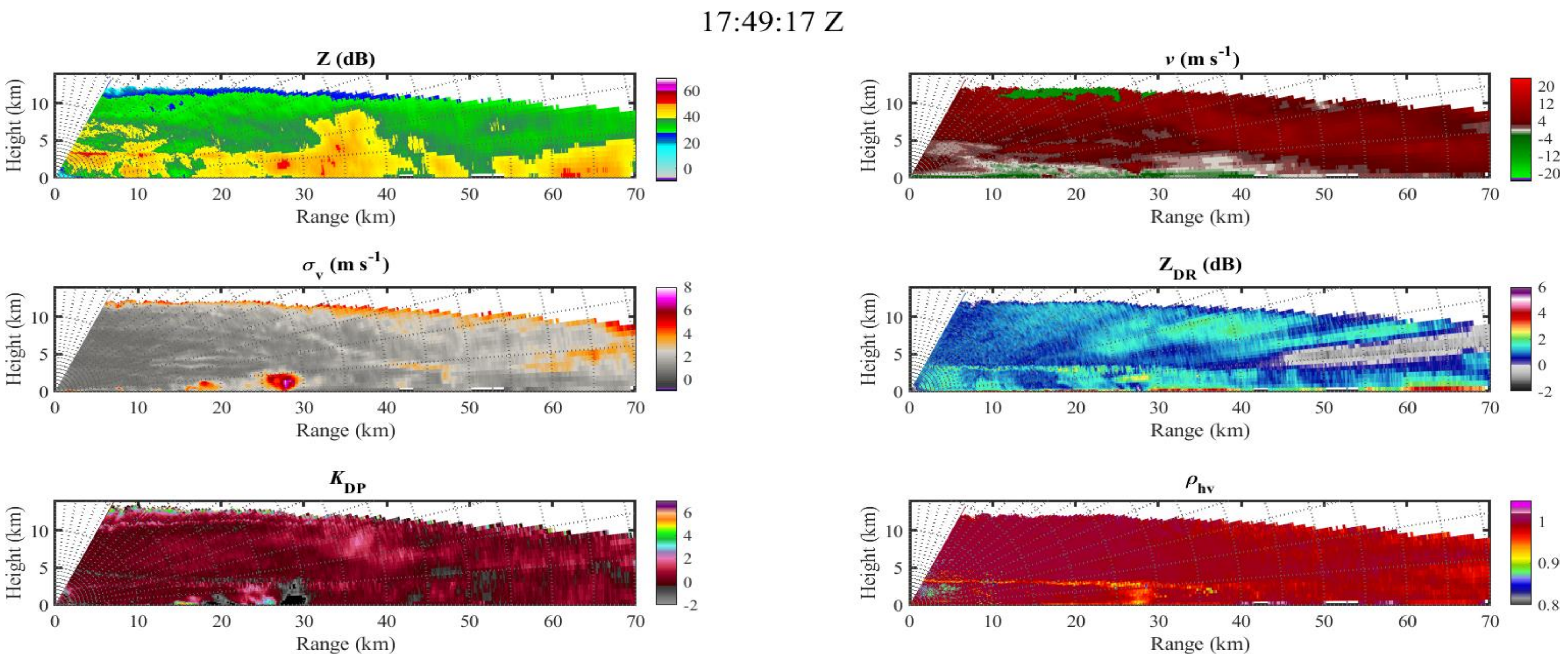

2021-09-30 17:50:26 - RHI at Az = 57

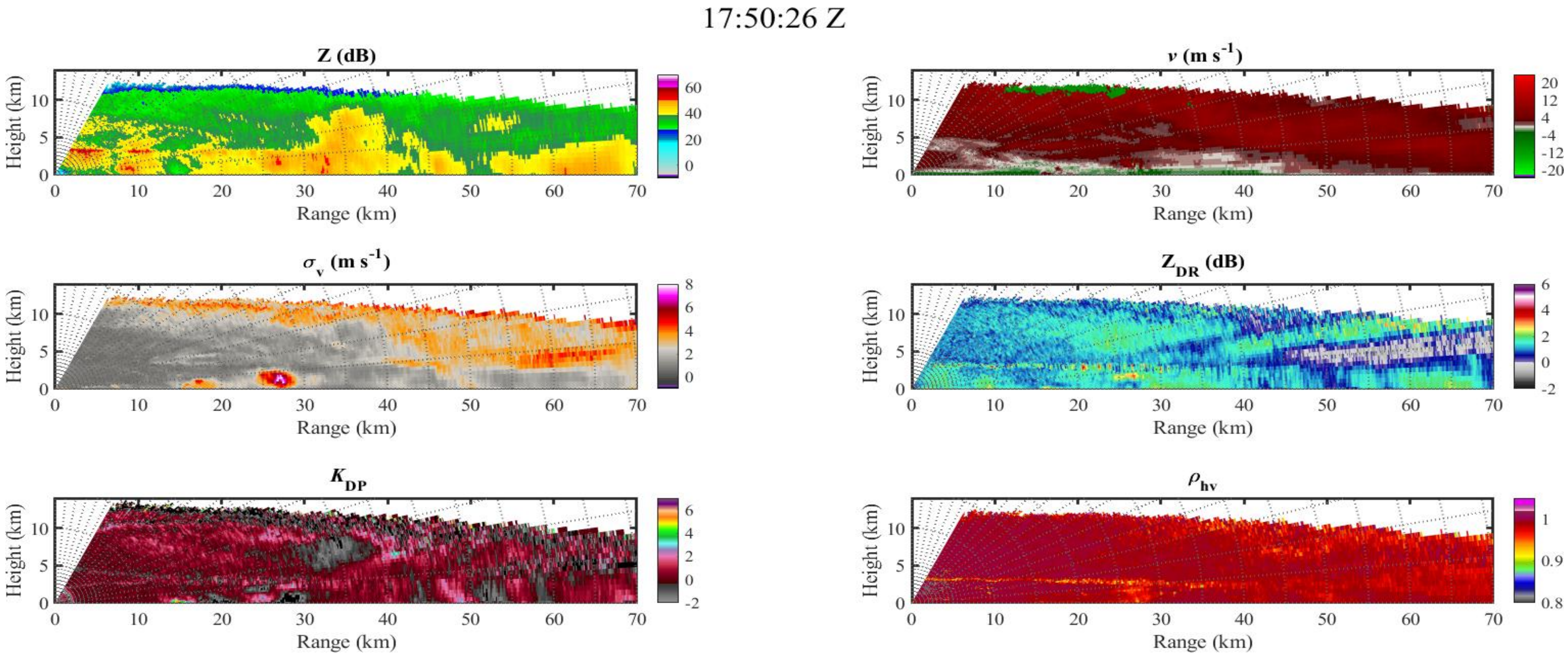

2021-09-30 17:50:30 - RHI at Az = 57

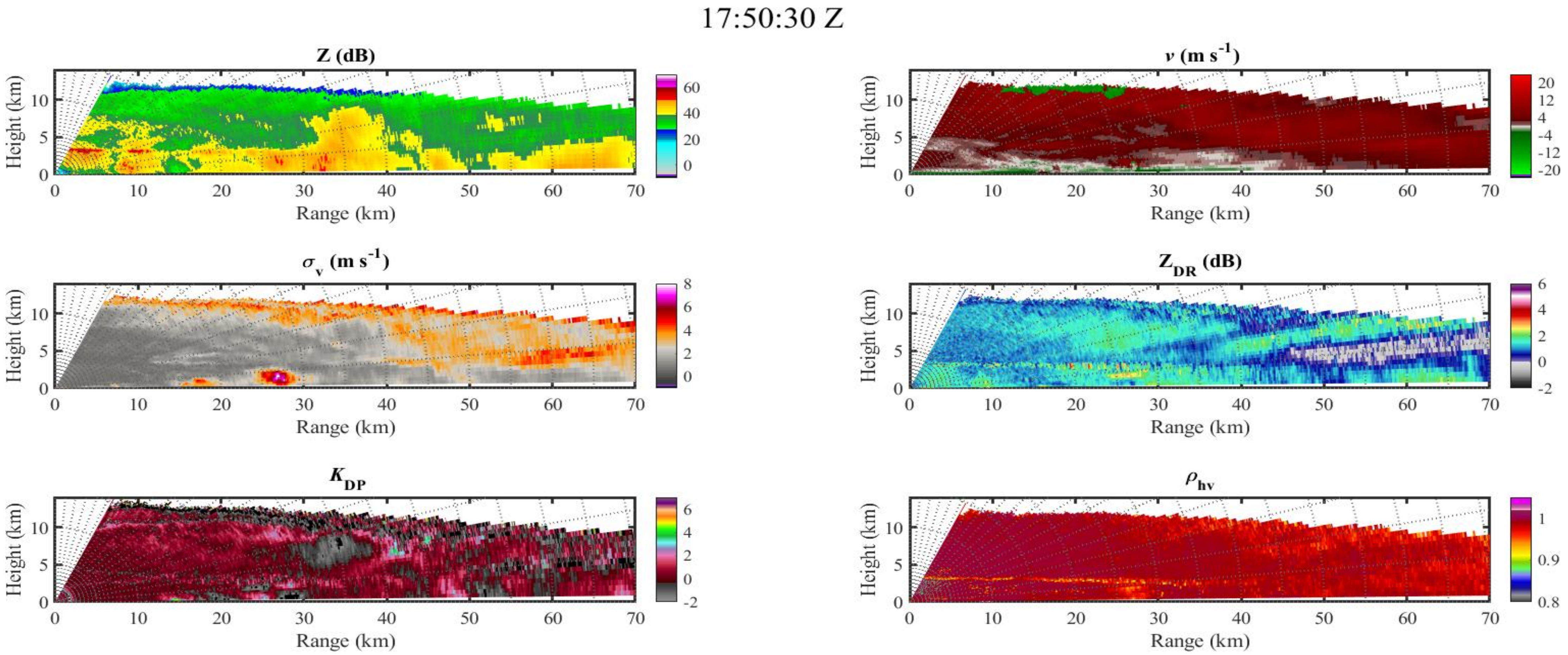

2021-09-30 17:50:35 - RHI at Az = 57

Courtesy of David Schvartzman